Earth-Science Reviews 129 (2014) 136–147

Contents lists available at ScienceDirect

Earth-Science Reviews

journal homepage: www.elsevier.com/locate/earscirev


# Paleo-$CO_2$ variation trends and the Cretaceous greenhouse climate

Yongdong Wang [a,*], Chengmin Huang [b], Bainian Sun [c], Cheng Quan [d,*], Jingyu Wu [a,c], Zhicheng Lin [e]

[a] Nanjing Institute of Geology and Palaeontology, Chinese Academy of Sciences, Nanjing 210008, China
[b] Department of Environmental Science and Engineering, Sichuan University, Chengdu 610065, China
[c] School of Earth Science, Lanzhou University, Lanzhou 730000, China
[d] Research Center of Paleontology and Stratigraphy, Jilin University, Changchun 130026, China
[e] Oil and Gas Engineering Institute, Chongqing University of Science and Technology, Chongqing 401331, China

ARTICLE INFO

*Article history:*
Received 24 July 2012
Accepted 3 November 2013
Available online 14 November 2013

*Keywords:*
Atmospheric $CO_2$
Cretaceous
Stomata index
Paleosol
Geochemical model
Greenhouse climate

ABSTRACT

The Cretaceous was one of the most remarkable periods in geological history, with a "greenhouse" climate and several important geological events. Reconstructions of atmospheric $CO_2$ using proxies are crucial for understanding the Cretaceous "greenhouse." In this paper we summarize the major approaches for reconstructing $CO_2$ based on paleobotanical or geochemical data, and synthesize the $CO_2$ variations throughout the Cretaceous. The results show that atmospheric $CO_2$ levels remained relatively high throughout the Cretaceous, but were lower in the early Cretaceous, highest in the mid-Cretaceous and gradually declined during the late Cretaceous. However, this overall trend was interrupted by several rapid changes associated with ocean anoxic events (OAEs) and the end-Cretaceous catastrophic event. New data on paleo-$CO_2$ levels from paleobotanical and paleosol evidences support not only the overall trends indicated by geochemical models, but provide more precise records of the short-term fluctuations related to brief episodes of climate change. Temporal resolution within the long quiet magnetic period in the middle Cretaceous is one of the obstacles preventing us from a more comprehensive understanding of the $CO_2$ climate linkage. But new paleo-$CO_2$ determinations and climatic data from stratigraphic sections of sediments intercalated with datable volcanic rocks will allow a better understanding of the relationships between fluctuations of atmospheric $CO_2$, climate change, and geological events.



**Contents**



## 1. Introduction

As one of the primary greenhouse gases, atmospheric $CO_2$ affects the surface temperature of the Earth, and is thought to be a major factor in global warming (Boucot and Gray, 2001; Royer, 2006; Fletcher et al.,

* Corresponding authors.
*E-mail addresses:* ydwang@nigpas.ac.cn (Y. Wang), quan@jlu.edu.cn (C. Quan).

0012-8252/$ – see front matter © 2013 Elsevier B.V. All rights reserved.
http://dx.doi.org/10.1016/j.earscirev.2013.11.001

2008). During the geological history of the last 450 Ma, global temperatures have co-varied with atmospheric $CO_2$ and it is considered the primary driver of Phanerozoic climate (Royer et al., 2004; Royer, 2008, 2010). Understanding paleo-$CO_2$ variations during the Earth's ancient greenhouse episodes are essential for predicting the response of climate to future elevated atmospheric $CO_2$ levels (Breecker et al., 2010).

The Cretaceous (145–65 Ma) represents one of the best examples of greenhouse climates in Earth history. As the greenhouse climate reached its summit in the mid-Cretaceous, the Earth was characterized by equably distributed warmth with mean annual polar temperatures exceeding 14 °C (Tarduno et al., 1998). There were no permanent polar ice sheets (Frakes et al., 1992), and sea levels were 100–200 m higher than those of today (Haq et al., 1987). During this time atmospheric $CO_2$ levels are estimated to have been 4 to 10 times higher than those prior to the Industrial Revolution (Cojan et al., 2000; Berner and Kothavala, 2001; Bice and Norris, 2002; Huber et al., 2002) and the Cretaceous Oceanic Red Bed (CORBS) are globally distributed (Wang and Hu, 2005; Wang et al., 2011).

More precise quantitative reconstructions of atmospheric $CO_2$ levels using terrestrial and marine records are critical for a better understanding of the "greenhouse" conditions of the Cretaceous, but proxy data for several of the stages of this period remain quite limited. In the past decade, an increasing number of paleo-$CO_2$ data have been reported for the Cretaceous. In this paper, we summarize the major approaches for paleo-$CO_2$ reconstructions for the Cretaceous, and review the progresses of paleo-$CO_2$ data collection from various parts of the world, covering different episodes during the Cretaceous. Using our comprehensive data compilation, we analyze the variations in atmospheric $CO_2$ during the Cretaceous, concentrating on critical intervals representing geological and biological events.

## 2. Major paleo-$CO_2$ reconstruction methods

For deep time, paleo-$CO_2$ can be inferred from either proxies or by the modeling of the long-term carbon cycle. Berner (1994) established the first model (GEOCARB) specifically designed to describe the evolution of atmospheric $CO_2$ levels during the entire Phanerozoic. Since then geochemical models have been refined (Ekart et al., 1999; Tajika, 1999; Berner and Kothavala, 2001; Wallmann, 2001; Hansen and Wallmann, 2003). During the last two decades a variety of proxies have been developed to reconstruct past atmospheric $CO_2$. These include fossil plant stomata (e.g. Beerling and Chaloner, 1993; McElwain and Chaloner, 1995; Kürschner et al., 1998; Royer, 2001; Kouwenberg et al., 2003; Konrad et al., 2008), stable carbon isotopes of paleosols (Cerling, 1991; Ghosh et al., 1995; Breecker et al., 2009; Huang et al., 2012), stable carbon isotopes of fossil liverworts (Fletcher, 2006; Fletcher et al., 2008), boron isotope pH's derived from marine carbonate microfossils (Hemming and Hanson, 1992; Pearson et al., 2009), and marine alkenones (Pagani et al., 1999; DeConto and Pollard, 2003; Pagani et al., 2005).

### 2.1. Paleo-$CO_2$ reconstruction using fossil stomata

The relationship between stomatal parameters of fossil leaves and paleo-$CO_2$ levels has been widely adopted as an effective tool for reconstructing atmospheric $CO_2$ levels of the past. Based on herbarium specimens, Woodward (1987) reported the negative correlation between the atmospheric $CO_2$ concentration and stomatal numbers. He demonstrated that both stomatal density (SD) (number of stomata per unit area of leaf) and stomatal index (SI) (percentage of leaf epidermal cells that are stomata) were inversely related to atmospheric $CO_2$ level during leaf development. This relationship is the basic principle that allows estimation of paleo-$CO_2$ by comparing the stomata of fossils to corresponding extant plants. The stomatal method offers the best temporal resolution of all paleo-$CO_2$ proxies (several months to $10^2$ years) (Royer et al., 2001a,b). It is considered to be the most suitable technique for detection of multi-millennial paleo-$CO_2$ perturbations in the geological record (Royer et al., 2001a,b) because the time resolution of the stomatal proxy is less than 100 years. The precision of the reconstructed paleo-$CO_2$ can be within ~10–40 ppm.

Four parameters are involved in the paleo-$CO_2$ reconstruction: 1) epidermal density (ED); 2) stomatal density (SD); 3) stomatal index (SI); and 4) the stomatal ratio (SR). The ED and SD are expressed as epidermal and stomatal numbers per $mm^2$. The SI is $[SD/(ED + SD)] \times 100$. The SR is the ratio of SIs between the fossil and its modern equivalent. Although both SD and SI respond to $CO_2$, SD increases under drought conditions because of a reduction in epidermal cell size, causing the stomata to be packed closer together (Salisbury, 1927; Beerling, 1996). Hence, SD is susceptible to fluctuations in the growing environment and is therefore a less reliable indicator of past $CO_2$ levels. In contrast, SI emphasizes the proportion of epidermal cells that are stomata. It is independent of epidermal cell size and measures stomatal initiation and development. It is not affected by subsequent cell expansion or contraction. SI is insensitive to changes in soil moisture supply, atmospheric humidity and temperature (Beerling, 1996) and is considered the best indicator for reconstruction of paleo-$CO_2$ using fossil plant cuticles. However, the epidermal cells can become difficult or impossible to count on poorly preserved fossil cuticles. Such fossil material requires the use of SD, with a suitable measure of caution (Beerling and Chaloner, 1993; McElwain and Chaloner, 1995).

Methodologically, the stomata-based paleo-$CO_2$ reconstructions can be subdivided into two categories: one based on comparison with the nearest living equivalent (NLE) and the other based on a regression function (RF). An NLE is a modern taxon that has a comparable ecological setting and/or structural similarity to its fossil counterpart. The SR (stomatal ratio) is defined as the stomatal index of the NLE to the fossil plant. SR values are related to the level of atmospheric $CO_2$ at the time when the NLE materials were collected (McElwain and Chaloner, 1995; McElwain, 1998). The NLE-based SR method has been used to make semi-quantitative estimates of paleo-$CO_2$ back to the Early Mesozoic and even into the Paleozoic (McElwain and Chaloner, 1995; Uhl and Herp, 2005). The SR method shows a pattern of paleo-$CO_2$ trends through geological time similar to those predicted from the GEOCARB geochemical models for the long-term carbon cycle (Royer et al., 2001a). It is assumed that a stomatal ratio of 1 is equal to either 300 ppm ($1\ SR = 2\ RCO_2$ — Recent standardization) or 600 ppm ($1SR = 2RCO_2$ — Carboniferous standardization) (McElwain and Chaloner, 1995). The Recent and Carboniferous standardizations are regarded as broad minimum and maximum estimates of paleo-$CO_2$.

Alternatively, the regression function of a particular taxon is derived from "greenhouse experiments" with the related modern plant. The regression function is based on the assumption that in the geological past the stomatal features of a plant responded to $CO_2$ change in the same way that they do today (Royer, 2001, 2003; Quan et al., 2010). Although experimental data are used to develop functions for comparison with pre-Quaternary fossil leaves, it turns out that in many cases the experimental growth conditions in a greenhouse produce results that are very different from those obtained from plants in the open. Cross calibration is required, e.g. by comparing the SI values of leaves grown at ambient $CO_2$ partial pressure with those grown under experimental conditions before combining the data sets (Royer et al., 2001a). To date, dozens of regression functions have been reported from diverse plant taxa (Table 1). However, the use of the RF method is largely limited to the Cenozoic because it requires that the taxon involved be a direct ancestor of the modern plant.

Considerable care is required in developing experimental 'training sets' for making paleo-$CO_2$ reconstructions. (A 'training set' is a collection of data on morphology of modern leaves and their growth environment that can be used to infer from measurements on fossils in the environmental conditions under which fossil plants lived.) Efforts are being made to obtain data from a wide range of plants with different

**Table 1**
Selected regress functions derived from herbarium or training set of modern plants for $CO_2$ reconstruction.

| | Regression function | Taxon based | Reference |
|---|---|---|---|
| 1. | $pCO_2 = \frac{(415\times SI-1961)\times 2000}{3337\times SI-20000}$ | *Ginkgo biloba* | Royer (2003) |
| 2. | $pCO_2 = \frac{52-SI-243}{1049\times SI-6250}\times 5000$ | *G. biloba* | Beerling et al. (2002) |
| 3. | $pCO_2 = \frac{1-0.1564\times SI}{0.00374-0.0005485\times SI}$ | *G. biloba* | Royer et al. (2001b) |
| 4. | $pCO_2 = \frac{70000\times(50\times SI-391)}{12301\times SI-100000}$ | *Metasequoia glyptostroboides* | Royer (2003) |
| 5. | $pCO_2 = \frac{SI-6.672}{0.003883\times SI-0.02897}$ | *M. glyptostroboides* | Royer et al. (2001a,b) |
| 6. | $pCO_2 = 10^{1.9624} - 0.4284 \times \log(SI)$ | *Ocotea foetens* | Kürschner and Kvaček (2009) |
| 7. | $pCO_2 = 10^{2.9567} - 0.4284 \times \log(SI)$ | *O. foetens* | Kürschner et al. (2008) |
| 8. | $pCO_2 = 10^{3.173} - 0.5499 \times \log(SI)$ | *Laurus nobilis* | Kürschner et al. (2008) |
| 9. | $pCO_2 = \frac{211.504\times SI-4053.26}{SI-24.8996}$ | *Stenochlaena palustris* | Beerling et al. (2002) |
| 10. | $pCO_2 = 419.48 - 7.6871 \times SI$ | *Neolitsea dealbata* | Greenwood et al. (2003) |
| 11. | $pCO_2 = \frac{SI-16.19}{0.0038}$ | *Tsuga heterophylla* | Kouwenberg et al. (2003) |
| 12. | $pCO_2 = 10^{3.1649} - 0.5055 \times \log(SI)$ | *Myrica cerifera* | Wagner et al. (2005) |
| 13. | $pCO_2 = 10^{2.973} - 0.3445 \times \log(SI)$ | *Osmunda regalis* | Wagner et al. (2005) |
| 14. | $pCO_2 = 10^{2.8861} - 0.317 \times \log(SI)$ | *Ilex cassine* | Wagner et al. (2005) |
| 15. | $pCO_2 = -63.902 \ln(SI) + 484.33$ | *Quercus robur* | van Hoof et al. (2008) |
| 16. | $pCO_2 = \frac{SI}{8.1309\times 10^{0.0009}}$ | *Callitris preissii* | Haworth et al. (2010) |
| 17. | $pCO_2 = \frac{SI}{-5.2908\times 10^{0.0022}}$ | *Callitris oblonga* | Haworth et al. (2010) |
| 18. | $pCO_2 = 559.67 - 27.447 \times SI$ | *Hypodaphnis zenkeri* | Barclay et al. (2010) |

genotypes growing under a variety of different environmental conditions (Birks et al., 1999; Royer et al., 2001a).

Some published data indicate a range of $CO_2$ values having little congruence, not only with those derived from geochemical methods, but also among different plant stomatal criteria (Yapp and Poths, 1992; Berner, 1997; McElwain et al., 1999; Retallack, 2001; Royer, 2001; Royer et al., 2001a; Tanner et al., 2001; Haworth et al., 2005). Paleobotanically, this inconsistency may be partly avoided by using multi-species analyses where different taxa show varying responses to $CO_2$ levels and $CO_2$ change. Mono-species-based paleo-$CO_2$ estimates are considered to be a more effective way to reduce the potential sources of error than multi-species approaches (Quan et al., 2009).

For the Cretaceous, the specific plant fossil groups used for reconstructing paleo-$CO_2$, based on either the RF- or NLE-method are ginkgos (Retallack, 2001; Chen et al., 2001; Beerling et al., 2002; Sun et al., 2007; Quan et al., 2009; Wan et al., 2011) and Cheirolepidiaceae and Cupressaceae conifers (Haworth et al., 2005; Passalia, 2009; Haworth et al., 2010).

### 2.2. Paleo-$CO_2$ reconstruction using paleosol carbonate

Pedogenic (soil) carbonate (calcite, $CaCO_3$) forms in soil where evaporation exceeds precipitation. This occurs typically in arid to subhumid regions that receive less than 800 mm of annual precipitation (Cerling, 1984; Royer et al., 2001a; Retallack, 2005). The carbonate ion incorporated into carbonates is predominantly derived from the atmospheric $CO_2$ that diffuses into the soil and the biological respired $CO_2$ produced by decomposition of organic matter in the soil, root respiration, etc., assuming the absence of groundwater $CO_2$ and $CO_2$ from carbonate weathering (Cerling et al., 1989; Quade et al., 1989; Royer, 2010). There is a marked difference in isotopic compositions of carbon in atmospheric $CO_2$ and biologically respired $CO_2$. In case of the variations of atmospheric $CO_2$ concentrations, the higher or lower partial pressure of isotopically heavier atmospheric $CO_2$ offsets changes due to the isotopically lighter respired $CO_2$, and the carbon isotopic value of pedogenic carbonate also accordingly rises or falls. The concentration of atmospheric $CO_2$ can be estimated from the known soil $CO_2$ concentration and the isotopic compositions of both sources (Cerling, 1991; Royer, 2010).

The pedogenic carbonate $CO_2$ paleobarometer developed by Cerling (1991) is expressed by the following equation (Cerling, 1999; Ekart et al., 1999):

$$Pa = Pr\,\frac{\left(\delta^{13}Cs - 1.0044\delta^{13}Cr - 4.4\right)}{\left(\delta^{13}Ca - \delta^{13}Cs\right)}$$

where $Pa$ is atmospheric $CO_2$ (ppm), $Pr$ is soil-respired $CO_2$ concentration (ppm) and $\delta^{13}Cs$, $\delta^{13}Cr$ and $\delta^{13}Ca$ are the stable carbon isotopic compositions of soil $CO_2$, soil-respired $CO_2$, and atmospheric $CO_2$, respectively.

The isotopic composition of biologically respired soil $CO_2$ ($\delta^{13}C_r$) is approximated by the $\delta^{13}C$ of paleosol organic carbon ($\delta^{13}C_o$) (Cerling, 1991). Consequently, the coexisting paleosol $\delta^{13}Co$ can be substituted for $\delta^{13}C_r$ in the model equation (Cerling, 1999). Fractionation of carbon isotopes induced by aerobic decomposition after burial of the paleosol can result in $\delta^{13}C$ enrichment by several per mil, so the organic carbon concentration in the paleosol must either approximate its maximum concentration in similar modern soils, or the paleosol organic matter must not enclose the $^{13}C$-enriched products of microbial decay in order to obtain a realistic $\delta^{13}C_o$ value (Wynn, 2007). The isotopic compositions of a well-preserved fossil terrestrial plants may be used as proxies for $\delta^{13}C_r$ instead of $\delta^{13}C_o$, but they are not abundant enough in paleosols to be able to construct a geological time series for paleo-$CO_2$ (Retallack, 2009a). An alternative method is to estimate $\delta^{13}C_a$ through geological time from $\delta^{13}C$ of planktic foraminifera from high resolution marine sediments (Pagani et al., 1999; Passey et al., 2002; Nordt et al., 2003; Retallack, 2009a), and calculate $\delta^{13}C_o$ using the equation proposed by Arens et al. (2000).

The isotopic composition of soil $CO_2$ ($\delta^{13}C_s$) is routinely derived from that of pedogenic carbonate ($\delta^{13}C_c$), corrected for temperature dependent fractionation following Romanek et al. (1992). To determine the temperature, one approach is to use an isotopic composition of oxygen in pedogenic carbonates ($\delta^{18}O_c$) representing modern climates (Dworkin et al., 2005; Prochnow et al., 2006). However, this method is questionable because of potential diagenetic effects on the oxygen isotopic composition of pedogenic carbonate after burial, the potential evaporative enrichment effects in arid climates (Cerling, 1984; Cerling

and Quade, 1993), and orographic rain-shadow effects (Kent-Corson et al., 2006; Retallack, 2009a).

The transfer function relating the molar ratios of $K_2O$ and $Na_2O$ to $Al_2O_3$ to mean annual temperature (Sheldon et al., 2002) was widely employed to infer paleotemperature (e.g., Kahniann and Driese, 2008; White and Schiebout, 2008; Retallack, 2009a,b; Retallack and Huang, 2011). However, considering the alteration of chemical composition by various pedogenetic processes and agents, not solely by temperature, this geochemical proxy should be applied cautiously in estimating paleotemperatures, particularly in paleosols developed under marsh, desert and tropical conditions (Nordt et al., 2006; Sheldon and Tabor, 2009).

The clumped-isotope carbonate paleothermometer is of potential utility despite the requirement of calibration for paleosols (Ghosh et al., 2007; Retallack, 2009a). Atmospheric $CO_2$ estimates scale directly with partial pressure of respired $CO_2$ in soil (Royer, 2010). Poorly constrained estimates of soil $CO_2$ for Cerling's (1991) pedogenic $CO_2$ paleobarometer limit the resolution in determining ancient $CO_2$ levels (Montañez et al., 2007; Leier et al., 2009; Retallack, 2009a; Breecker et al., 2010; Huang et al., 2012). Commonly, the $P_r$ value is given within wide limits, such as 5000 or 10,000 ppm (Leier et al., 2009).

For much of the geologic past, estimates of paleo-$CO_2$ using different methods are generally consistent (Royer, 2006). The major exception is the paleosol carbonate proxy, whose $CO_2$ estimates are often more than twice as high as coeval estimates from other methods. This discrepancy has led some to question the validity of the other methods and has hindered attempts to understand the linkage between paleo-$CO_2$ and other parts of the Earth's system (Royer, 2010). Breecker et al. (2010) break important new ground for resolving this conflict, and have contributed significantly towards improving one of the more popular paleo-$CO_2$ proxies (Royer, 2010). They point out that paleo-$CO_2$ concentrations calculated using the paleosol barometer are overestimates by a factor of two or more because of the arbitrary assumption of ~5000–10,000 ppm for soil $CO_2$ concentrations rather than $P_r = 2,500$ ppm (Breecker et al., 2010). The higher range was primarily based on a mean growth season $CO_2$ concentrations in modern soils that do not contain pedogenic carbonate.

Carbonate precipitation in soils is highly seasonal, so assumptions based on a yearly average are likely to be incorrect (Breecker et al., 2010). It is an oversimplification to assume the "best guess" value of 2500 ppm for soil $CO_2$ concentration in all cases (Royer, 2010). Soil $CO_2$ concentrations are highly variable; they differ in diverse soils and at different depths. Furthermore, within a soil profile different proportions come from the atmosphere and from biogenic respiration. A refined proxy for estimating the soil $CO_2$ level is the transfer function between soil $CO_2$ and the depth to the calcic horizon (Retallack, 2009a); it incorporates the variations of productivity, porosity and other variables with soil depth, and may provide a higher resolution estimate of the paleo-$CO_2$ concentration (Royer, 2010; Huang et al., 2012).

### 2.3. Relevant geochemical methods

Berner et al. (1983) proposed the first geochemical model (which became known informally as the BLAG model) relating carbonates, silicates and atmospheric $CO_2$ concentrations over the past 100 Ma. Berner (1991) proposed a more comprehensive model, now known as GEOCARB I, for calculating the atmospheric $CO_2$ levels during all of Phanerozoic time, the past 570 Ma, based on inputs of geological, geochemical, biological, and climatological data. Berner (1994) revised and improved this as GEOCARB II. In this model the decrease of atmospheric $CO_2$ values during the Mesozoic differs from the results of GEOCARB I. Berner and Kothavala (2001) made a further revision, GEOCARB III. It shows an overall pattern similar to that of GEOCARB II, with very high $CO_2$ values during the early Paleozoic, followed by a large drop during the Devonian and Carboniferous, and then a rise to moderately high values during the Mesozoic, followed by a gradual decline through both the late Mesozoic and Cenozoic. These geochemical models are incapable of delimiting shorter term $CO_2$ fluctuations (e.g. late Ordovician glaciation, Paleocene–Eocene boundary) because the input data are 10 Ma or longer averages. Nevertheless, both GEOCARB II and GEOCARB III indicate an overall trend of paleo-$CO_2$ showing a correlation with paleotemperatures derived from other data. They provide clear support for the concept of an atmospheric greenhouse effect driven by $CO_2$.

More recently, a new model, GEOCARBSULF, has been constructed for the combined long-term cycles of carbon and sulfur (Berner, 2006). It shows little overall change in the curves of $CO_2$ over time from the earlier GEOCARB models and isotope mass balance modeling. Bergman et al. (2004) have also presented a model of biogeochemical cycling over Phanerozoic time: COPSE (Carbon–Oxygen–Phosphorus–Sulfur Evolution). Both GEOCARBSULF and COPSE show a Late Paleozoic minimum of paleo-$CO_2$, but their results for the Mesozoic and Cenozoic (the past 250 Ma) differ considerably. The Phanerozoic paleo-$CO_2$ estimates from the COPSE model differ from GEOCARB in that there is a broad minimum of paleo-$CO_2$ in the Triassic, a gentle rise to a peak in the Cretaceous and a decline over the past 100 Ma. GEOCARB III indicates a paleo-$CO_2$ peak in the middle Jurassic and a decrease since that time.

Fletcher et al. (2004, 2006, 2008) tested the potential of fossil bryophyte isotopes as a new pre-Quaternary paleo-$CO_2$ proxy. They found that carbon isotope discrimination ($\Delta^{13}C$) by bryophytes (liverwort and moss) shows a positive relation with paleo-$CO_2$ level. An extended model of bryophyte carbon isotope discrimination, BRYOCARB, was set up to integrate the biochemical theory of photosynthetic $CO_2$ assimilation with controls on $CO_2$ supply by diffusion from the atmosphere (Fletcher, 2006; Fletcher et al., 2006). Using this model, Fletcher et al. (2008) show that fossil bryophytes provide a more coherent record of fluctuations in the Earth's atmospheric $CO_2$ levels over the Mesozoic and early Cenozoic than other techniques in the same interval. However, as a new paleo-$CO_2$ proxy, it is less widely utilized; more data on fossil bryophytes should be used to estimate paleo-$CO_2$ and reduce the uncertainties in the geological past (Beerling and Royer, 2011). As bryophytes are normally small and delicate, some of them are not easily fossilized and their remains may be ignored by the researchers so that, compared to higher plants, there are not many records of fossil bryophytes. Nevertheless, at least two benefits of the bryophyte BRYOCARB model have been recognized: 1) they are systematically independent and the preliminary experiments are simpler than those for the stomatal proxy; 2) as one of the earliest land plants (Wellman et al., 2003; Wellman, 2010), their geological time span is longer than most other proxies so that it is possible to get a long paleo-$CO_2$ curve using this technique.

Geochemical models provide paleo-$CO_2$ estimates for the entire Phanerozoic, but most provide 5–10 Ma mean values. They do not often resolve short-term excursions. The error estimates for geochemical models range from $\pm$70–200 ppm for the Tertiary to as much as $\pm$300 ppm for the Paleozoic (Royer et al., 2001a). Geochemical models are very important for reconstructing the general trends of the background paleo-$CO_2$ level during geological history but other proxies need to be used to detect the short-term variations of atmospheric $CO_2$.

## 3. Paleo-$CO_2$ variations in the Cretaceous

Estimates of Cretaceous atmospheric paleo-$CO_2$ levels have been published for a variety of localities in North and South America, Europe, and Asia, based on either stomata or isotope analysis. In addition, several geochemical models also estimate the trend of Cretaceous $CO_2$ levels (e.g., Tajika, 1999; Wallmann, 2001; Berner and Kothavala, 2001; Berner, 2006). The data cover the geological intervals from Berriasian–Valanginian and Hauterivian–Albian of the Early Cretaceous, and Cenomanian–Turonian, Coniacian–Campanian and Maastrichtian of the Late Cretaceous, as well as some remarkable events in the

Cretaceous: the Ocean Anoxic Events (OAEs) and Cretaceous–Tertiary Boundary (KTB). The major results, based on analysis of fossil stomata and paleosol isotopes are summarized and listed in Table 2. They are plotted in Fig. 1 along with results from geochemical models and other isotope studies.

### 3.1. Early Cretaceous paleo-$CO_2$ variations

Several studies have been carried out to reconstruct Early Cretaceous paleo-$CO_2$ based either on paleosols (Robinson et al., 2002; Leier et al., 2009; Huang et al., 2012) or fossil plants compared with their nearest living equivalents (Retallack, 2001; Chen et al., 2001; Beerling et al., 2002; Haworth et al., 2005; Sun et al., 2007; Passalia, 2009; Barclay et al., 2010). For Berriasian to Valanginian time two studies have been undertaken, based on the fossil *Ginkgo coriacea* from the Early Cretaceous Huolinhe Formation in northeastern China. Chen et al. (2001) reported a $RCO_2$ of 2.8 (840 ppm), similar to the $RCO_2$ of 2.55–3.20 (765–960 ppm) determined by Sun et al. (2007) for the Berriasian. ($RCO_2$ is defined as the ratio of the mass of $CO_2$ in the atmosphere at some time in the past to a pre-industrial value assumed to be 300 ppm). Sun et al. (2007) proposed that during the Berriasian the paleo-$CO_2$ increased from ~1530 ppm in the early Berriasian to 1920 ppm in the late Berriasian (Fig. 1). From the local geology they linked the Berriasian paleo-$CO_2$ increase to the Yanshanian movement during the Early Cretaceous that produced intense volcanic activity. They noted that the plant-based results essentially agree with those of GEOCARB III of Berner and Kothavala (2001). All of the results lie below the median line but are within the error envelope. However, taking all available geochemical models into account, their results are in closer agreement with those of Tajika (1999) (Fig. 1).

There are few data on atmospheric paleo-$CO_2$ for the earliest stages of the Early Cretaceous from paleosol carbonates. Recent calculations of paleo-$CO_2$ levels from Chinese paleosols (Huang et al., 2012) suggest that the paleo-$CO_2$ levels were low during the early-middle Berriasian, 389 ppm at most and an average of 360 ppm. There is also a mean value of at most 241 ppm in the early Valanginian (Huang et al., 2012) (Fig. 1). By contrast, Cerling (1991) reported an atmospheric $CO_2$ concentration range from 1600 ppm to 3300 ppm in the Early Cretaceous based on pedogenic carbonates. Fluctuations between 1700 ppm, 3200 ppm and 2300 ppm were calculated from late Valanginian and Hauterivian based on paleosol carbonates in Japan and southeast Korea (Lee, 1999; Lee and Hisada, 1999), respectively. Paleo-$CO_2$ estimates based on paleosols from Liaoning in Northeast China show a range during the late Barremian between 365 ppm and 644 ppm with an average of 530 ppm (126 Ma) (Huang et al., 2012). A Barremian–Aptian $CO_2$ level was estimated by Retallack (2009b) to be 400 ppm (126 Ma), inferred from *Ginkgo* stomatal index, but an average $CO_2$ concentration for that time of 1478 ppm (125 Ma) was suggested using data from carbonate paleosols of South Asia (Leier et al., 2009).

Haworth et al. (2005) made estimates of paleo-$CO_2$ variations during the Hauterivian to Albian (Early Cretaceous) from the UK and USA based on multi-NLEs of the extinct Cretaceous conifer *Pseudofrenelopsis parceramosa*. They used the ratio between stomatal indices of fossil cuticles and those from four modern NLEs. Their results indicate a relatively long-term low and only slightly varying paleo-$CO_2$ over the Hauterivian–Albian interval, a low of ~560–960 ppm in the early Barremian and a high of ~620–1200 ppm in the Albian. These results are largely consistent with GEOCARB II.

Using the carbon isotope composition of calcrete nodules, Robinson et al. (2002) estimated a similar paleo-$CO_2$ of 560 ppm for the early Barremian from the same bed of the Wealden Group in southern England. However, Retallack's (2001) paleo-$CO_2$ reconstruction, based on stomatal indices of fossil ginkgoales using modern *Ginkgo biloba* for calibration, differs from the above record. The recalibrated results of paleo-$CO_2$ using the NLE approach demonstrate a close agreement between Retallack's ginkgoales-based estimates and those of the *Pseudofrenopsis* conifers (Haworth et al., 2005).

Another suite of paleo-$CO_2$ estimates was reported by Passalia (2009), based on stomatal frequency analysis of several Early Cretaceous fossil conifers and ginkgoalean taxa from Patagonia, Argentina. These indicate that the atmospheric $CO_2$ content was similar during the middle Aptian but may have become slightly higher during the late Albian–early Cenomanian (Passalia, 2009). The $CO_2$ content estimated from the conifers ranges between ~700 and 1400 ppm. This is 2–4 times higher than at present, and is consistent with those predicted previously. The paleo-$CO_2$ level indicated by the middle Aptian conifers is generally higher than the range determined from ginkgoales in Patagonia. The $CO_2$ estimates from conifers are based on more extensive and complete data sets than those of the ginkgoales (Passalia, 2009).

For the Early Cretaceous the paleosol paleobarometer estimates vary from ca. 241 ppm to ca. 3200 ppm, because of different assumptions (Boucot and Gray, 2001; Leier et al., 2009; Retallack, 2009a). The discrepancy is largely due to the assumed values of soil $CO_2$. These conflicting results for Early Cretaceous paleo-$CO_2$ levels estimated from stomatal indices and paleosol carbonates are shown in Fig. 1. Early Cretaceous $CO_2$ concentrations were very low based on the paleosol data of Huang et al. (2012), and indicate that not all of the

**Table 2**
Major results using fossil stomata and paleosol proxy data from the Cretaceous deposits.

| Age | Stages | Estimated paleo-$CO_2$ results (ppm) | Proxy or methods | Locality | References |
|---|---|---|---|---|---|
| Late Cretaceous | Maastrichtian | 530, 590–550–592 | Stomata | NE China | Quan et al. (2009) |
| | Campanian | 531–620 | Stomata | NE China | Quan et al. (2009) |
| | Santonian | 661–531–565 | Stomata | NE China | Wan et al. (2011) |
| | Coniacian–Turonian | 680–630–970–520 | Stomata | NE China | Wan et al. (2011) |
| | Cenomanian | 37–2000–500 | Stomata | USA | Barclay et al. (2010) |
| | | 700–1400 | Stomata | UK, USA | Haworth et al. (2005) |
| | | 1000–1400 | Liverwort isotope | Antarctica | Fletcher et al. (2006) |
| Early Cretaceous | Albian | ~620–1200 | Stomata | UK, USA | Haworth et al. (2005) |
| | Aptian–Barremian | 700–1400 | Stomata | Argentina | Passalia (2009) |
| | | 400, 1478 | Stomata | USA | Retallack (2009a,b) |
| | | 365–(530)–644 | Paleosol | NE China | Huang et al. (2012) |
| | | 560–960 | Stomata | UK, USA | Haworth et al. (2005) |
| | | ~560 | Paleosol | UK | Robinson et al. (2002) |
| | Hauterivian–Valanginian | 1700–3200 | Paleosol | Japan, Korea | Lee (1999), Lee and Hisada (1999) |
| | | 740 ($RCO_2$ 2.8) | Stomata | China | Chen et al. (2001) |
| | | 241 | Paleosol | China | Huang et al. (2012) |
| | Berriasian | 389 (360) | Paleosol | China | Huang et al. (2012) |
| | | 765–960 ($RCO_2$ 2.55–3.2) | Stomata | China | Sun et al. (2007) |
| | | ~1530–1920 | Stomata | China | Sun et al. (2007) |

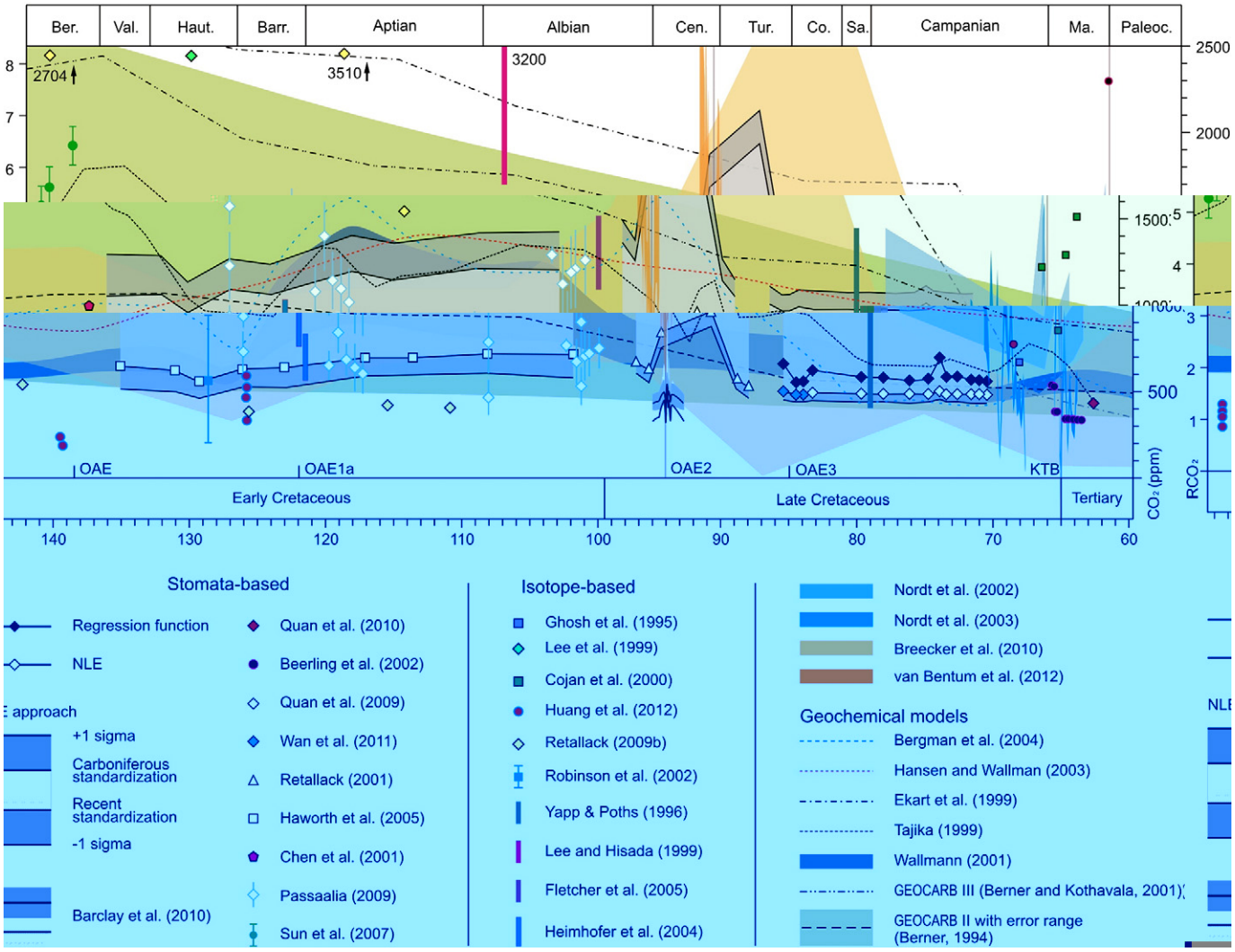


**Fig. 1.** Cretaceous paleo-$CO_2$ reconstructions based on plant fossil, isotope and geochemical models.

Cretaceous was a $CO_2$ greenhouse episode. This result is supported by the paleo-$CO_2$ estimates of Robinson et al. (2002) inferred from Barremian pedogenic carbonates in England. It is also supported by the studies of Haworth et al. (2005) using the stomatal index of fossil plants and Retallack's (2009b) paleosols. The proposition of higher levels of atmospheric $CO_2$ during the Early Cretaceous than those of the Late Cretaceous and Early Eocene (Cerling, 1991, 1992; Sinha and Stott, 1994) is in disagreement with the geological climatic data. Their atmospheric $CO_2$ levels for that period were overestimates (Boucot and Gray, 2001).

A reduction in sea-floor spreading rates and/or increase in continental weathering from the Late Jurassic to the mid-Cretaceous and burial of organic carbon during OAEs are thought to have contributed to low atmospheric paleo-$CO_2$ concentrations between episodes of high atmospheric $CO_2$ (Robinson et al., 2002; Gröcke et al., 2005).

### *3.2. Late Cretaceous paleo-$CO_2$ variations*

Late Cretaceous paleo-$CO_2$ levels have been mainly deduced from fossil stomatal analysis in USA, Argentina and China (Passalia, 2009; Quan et al., 2009, 2010; Barclay et al., 2010; Wan et al., 2011) and geochemical models (e.g. Berner, 1994; Tajika, 1999; Berner and Kothavala, 2001; Fletcher et al., 2006). Barclay et al. (2010) reported an increase by ~20% over the background level of 370 ppm in Cenomanian, and a decrease up to 26% in the Turonian based on fossil stomatal analysis of the family Lauraceae. Isotope analysis on fossil liverworts, from Alexander Island, Antarctica, indicates an early Cenomanian paleo-$CO_2$ level of 1000–1400 ppm (Fletcher et al., 2006). This value is consistent with independent proxy data and long-term carbon cycle models (Fletcher et al., 2006). It is also supported by recalibrated stomatal data of conifers and ginkgoales from the Southern Hemisphere (Passalia, 2009), which indicate a $CO_2$ range between 700 and 1400 ppm for the Cenomanian.

Recently, Wan et al. (2011) recalculated Retallack's (2001) original ginkgoalean data for paleo-$CO_2$ during the Cenomanian to Coniacian. The recalculated results illustrate a series of dramatic changes during this interval (Fig. 1). In the mid-Cenomanian to late Turonian, the $CO_2$ content declined from ~680 ppm to ~630 ppm, followed by a rebound up to 970 ppm. Then began a continuous $CO_2$ decrease to ~520 ppm in the mid-Coniacian. Although with drastic fluctuations, as illustrated in Fig. 1, the recalibration results show an overall decline from the mid-Cenomanian (~680 ppm) to mid-Coniacian (~520 ppm).

A sharp decline in atmospheric $CO_2$, from ~970 ppm to ~520 ppm, from the late Turonian to mid-Coniacian has a resolution of about 1 Ma. It is not recognized in most geochemical models except that of Berner (2004). The fluctuations of the recalibrated data match well with Tajika (1999) in the mid-Turonian to early Coniacian. However, it should be noted that the late Cenomanian to mid-Turonian $CO_2$ trend is opposite to that of geochemical data, which shows a decline (Fig. 1). A more detailed evidence is needed to confirm the $CO_2$ levels

during this interval. Although no paleobotanical data are available for the late Coniacian, it appears that there is a slightly declining trend during this interval (Fig. 1).

Using the stomatal index technique, Wan et al. (2011) and Quan et al. (2009) reconstructed $CO_2$ levels in the Santonian through Campanian by both RF and NLE methods based on one fossil species, *Ginkgo adiantoides*, from a single profile. In comparison to multispecies-based $CO_2$ reconstructions, the monospecies-based reconstruction minimizes potential bias produced by data using different species, because the stomata-$CO_2$ response is species-specific (Royer, 2001; Beerling and Royer, 2002; Haworth et al., 2010, 2011). RF-based $CO_2$ estimates from the SI analyses vary from ~661 ppm in the early Santonian to ~531 ppm in the middle and ~565 ppm in the late Santonian. The NLE-based $CO_2$ reconstructions closely agree with the RF-based results, and indicate that the atmospheric $CO_2$ content declined from the early Santonian (~503 ppm) to a minimum in the mid-Santonian (~478 ppm), and then rebounded slightly in the late Santonian (~486 ppm) (Wan et al., 2011). Despite the slightly higher estimates using the RF method (~97 ppm on average), the two sets of stomata-based results suggest a modest decrease of $CO_2$ throughout the Santonian (Fig. 1). These Chinese data for Santonian $CO_2$ content are compatible with the levels estimated by GEOCARB II of Berner (1994). However, GEOCARB III (Berner and Kothavala, 2001) predicts a Santonian $CO_2$ value of about 1270 ppm, which is much higher than the Chinese proxy data, although those values (both RF- and NLE-based) lie in the overall range of GEOCARB II and III.

High resolution estimates of paleo-$CO_2$ levels from mid-Santonian to early Campanian have been proposed based on Chinese fossil *Ginkgo* stomatal data. These show a rapid rise, from ~531 to ~620 ppm (Quan et al., 2009). However, this needs to be confirmed because the earliest Campanian paleo-$CO_2$ estimate was based only on a single fossil *Ginkgo* specimen. From this interval onward, the $CO_2$ levels show a long-term gradual decrease, from ~590 to 550 ppm, with the exception of a short fluctuation (up to ~690 ppm) in the late Campanian. This short-term $CO_2$ peak is followed by a rapid return to background values of 592 ppm (Fig. 1). This rise and fall represents a real short-term carbon dioxide fluctuation of paleo-$CO_2$. Similar fluctuations have been recognized in critical vegetation turnover intervals, such as at the Triassic–Jurassic boundary (McElwain et al., 1999), at the Cretaceous–Tertiary boundary (Beerling et al., 2002), at the Paleocene–Eocene boundary (Royer et al., 2001b), and at the early-middle Miocene transition (Kürschner et al., 2008). All of these suggest short-term coupling between atmospheric $CO_2$ and coeval geological events. After the late Campanian $CO_2$ fluctuation, there appear to be no sudden changes in paleo-$CO_2$ during the Maastrichtian. The atmospheric $CO_2$ level gradually decreased to 530 ppm until the K–T boundary event (Beerling et al., 2002; Beerling and Royer, 2002; Royer et al., 2007) (Fig. 1).

Geochemical studies predict that atmospheric $CO_2$ levels underwent a long-term decline through the Late Cretaceous (Berner, 1994; Ekart et al., 1999; Tajika, 1999; Berner and Kothavala, 2001; Wallmann, 2001), from about 1975 ppm to 450 ppm (Fig. 1). Recent RF-based paleobotanical results also indicate a declining trend in $CO_2$ content with a magnitude of ~100 ppm, but showing several fluctuations (Fig. 1). These are not recognized by the geochemical results, probably because of the different resolutions of the two approaches.

Wallmann (2001) reported on the results of a box model for the Cretaceous to Cenozoic global carbon–calcium strontium cycle. This model accounts for carbon masses in ocean and atmosphere, in carbonate, and in particulate organic carbon (POC). According to Wallmann (2001), the high Ca concentrations during the Cretaceous reflect the decline of atmospheric $CO_2$, because of the negative feed-back provided by POC burial, which is coupled to $CO_2$-dependent weathering rates. For the Late Cretaceous, his model shows a downward trend of atmospheric $CO_2$, from Cenomanian to Campanian. However, the stomata-based results from China indicate that $CO_2$ declined more rapidly from the early to middle and late Santonian (Wan et al., 2011).

## 4. Cretaceous paleo-$CO_2$ and major geological events

The Cretaceous represents one of the most remarkable periods of geologic history. It was not only a long greenhouse episode, but several unusual geological phenomena occurred: the Oceanic Anoxic Events (OAEs) (Schlanger and Jenkyns, 1976; Wang et al., 2005) and the K–T boundary catastrophe (KTB) (Alvarez et al., 1980). These triggered rapid environmental and climate changes and had profound impacts on the biosphere (McElwain et al., 2005; Davis et al., 2009; Royer et al., 2007). They have also been linked to variations of paleo-$CO_2$.

### 4.1. Paleo-$CO_2$ of the Ocean Anoxic Events (OAEs)

The most dramatic environmental changes during the Cretaceous concerned the oxidation state of the ocean, recognized as the "Oceanic Anoxic Events" (OAEs). OAEs were first described by Schlanger and Jenkyns (1976) as global-scale transient periods of marine anoxia, accompanied by the widespread deposition of organic carbon-rich sediments, occurring at the Aptian–Albian and Cenomanian–Turonian boundaries. Subsequent studies on sedimentary sections across the globe have expanded the stratigraphic record of such events. The major anoxic intervals were the Weissert OAE in the late Valanginian, the early Aptian Selli event (OAE1a), at the Cenomanian–Turonian boundary (OAE2, Bonarelli event), and the Coniacian–Santonian event (OAE3) (Leckie et al., 2002; Erba, 2004). OAEs are believed to have been associated with major perturbations in the global carbon cycle. They show significant $\delta^{13}C$ excursions, both positive and negative (Arthur et al., 1988). They are represented by organic-rich sediments ("black shales") and were often accompanied by biotic extinctions (Leckie et al., 2002).

OAEs were often succeeded by deposition of Fe-oxide-rich "Oceanic Red Beds" (CORBs) (Hu et al., 2005; Wang et al., 2005; Hu et al., 2006, 2009; Wang et al., 2011). Brief episodes of CORB deposition occurred after the mid-Cretaceous OAEs in the Tethyan Realm (e.g. Hu et al., 2006); some of them are correlated with cold episodes (Wagreich et al., 2009a,b). Following OAE 2, CORBs became common throughout the deep ocean.

The early Aptian OAE1a (*ca.* 120 Ma) represents the first globally distributed black shale event of the Cretaceous and is regarded as a major turning point of mid-Cretaceous paleoceanography (Gröcke et al., 1999; Jenkyns, 1999, 2003; Heimhofer et al., 2004). OAE1a is accompanied by dramatic turnovers in calcareous nannoplankton (Erba, 1994) and by high extinction and origination rates of siliceous and calcareous plankton (Erbacher and Thurow, 1997; Leckie et al., 2002). The deposition of organic-rich sediments during the Early Aptian OAE1a has been interpreted as resulting in a major decrease of atmospheric $CO_2$ concentrations. Haworth et al. (2005) documented a relatively low and only slightly varying paleo-$CO_2$ over the Hauterivian–Albian interval; it apparently lacked the large-magnitude rapid fluctuations in paleo-$CO_2$ of later times. However, due to the sparse nature of the sampling, their results have a low resolution across the OAE1a event, and thus could not delimit a pronounced variation of $CO_2$ associated with this event. By contrast, Heimhofer et al. (2004), using carbon isotope values of presumed algal biomarkers, inferred a paleo-$CO_2$ excursion during the OAE1a event of 840–1120 ppm. After OAE1a, the paleo-$CO_2$ decreased to about 714–950 ppm (Fig. 1), reflecting a 10–15% reduction in the level of atmospheric $CO_2$. This sharp decline of $CO_2$ happens within 1 Ma across the OAE1a event boundary sampled with a high resolution. It reflects the close relationship between paleo-$CO_2$ and the OAE1a event.

The relatively low paleo-$CO_2$ levels (even in the Aptian–Albian interval) and the reduction in paleo-$CO_2$ after OAE1a is consistent with compilations of oxygen isotope data (Veizer et al., 2000; Weissert and Erba, 2004), which indicate a relatively cool mid-Cretaceous.

The Cenomanian–Turonian OAE2, the Bonarelli event, is the classic example and probably the best-studied of the OAEs. It is characterized

by global deposition of organic-rich sediments (Schlanger and Jenkyns, 976; Jenkyns, 2003) accompanied by a positive carbon isotope excursion in bulk organic matter of 4‰ and in marine carbonates of 2–3‰. To reconstruct the paleo-$CO_2$ across OAE2, Barclay et al. (2010) incorporated NLE with the RF method. For counting stomatal frequency of dispersed leaf cuticle from a paralic facies in Utah, USA, that brackets the OAE2 interval, they selected *Laurus nobilis* and *Hypodaphnis zenkeri* of the family Lauraceae as the NLE of the mother plants of the dispersed cuticle types. They used the published transfer function for *L. nobilis* and the training set function of *H. zenkeri* to estimate paleo-$CO_2$ across OAE2. Their results have a resolution of about 2 Ma. The paleo-$CO_2$ increased by ~20% over the background level of ~370 ppm immediately before the onset of OAE2, but dramatically dropped by up to 26% during OAE2. This was followed by two peaks of paleo-$CO_2$ rebound immediately after the event (Fig. 1). A similar paleo-$CO_2$ pattern across OAE2 was observed in phytane carbon isotope records from ODP Site 1260 in Demerara Rise of western Atlantic (van Bentum et al., 2011) (Fig. 1), suggesting that the lowered paleo-$CO_2$ at OAE2 is in response to enhanced organic matter burial. The paleo-$CO_2$ peaks before and after the event are responses to coeval volcanism and magmatic activity (Barclay et al., 2010; van Bentum et al., 2011).

### 4.2. Paleo-$CO_2$ across the Cretaceous–Tertiary boundary

The catastrophic event that occurred at the Cretaceous–Tertiary boundary (KTB), about 65 Ma ago, resulted in one of the five largest mass extinction events in the Earth's history. It profoundly influenced the course of biotic evolution (Hsü et al., 1982; Benton, 1995). The extinctions coincided with a major extraterrestrial impact event and massive volcanism in India. Determining the importance of the event as a driver of environmental and biotic change across the Cretaceous–Tertiary boundary (KTB) depends on constraining the mass of $CO_2$ injected into the atmospheric carbon reservoir (Beerling et al., 2002). The two hypotheses to explain this biotic crisis attribute it either to outgassing of $CO_2$ during eruption of the Deccan Traps in India (Courtillot et al., 1986; Officer et al., 1987) or to $CO_2$ release from carbonate rocks by impact of an extraterrestrial object (Alvarez et al., 1980).

It has taken some time to evaluate the magnitude of the $CO_2$ fluctuation through the KTB. Paleobotanical studies show that up to 57% of plant species were wiped out at the KTB (Johnson et al., 1989; McIver, 1999; Wilf and Johnson, 2004; Ocampo et al., 2006; Nichols and Johnson, 2008). Other taxa survived the catastrophe probably due to their special ecological niche or refuges (Tschudy et al., 1984). They allow estimation of the atmospheric $CO_2$ change across the boundary using the stomatal technique.

Using the reverse relationship between paleo-$CO_2$ and the stomatal index of land plant leaves, Beerling et al. (2002) reconstructed atmospheric $CO_2$ concentrations across the KTB based on fossil cuticles of *Ginkgo* and the fern *Stenochlaena*. By calibrating regression functions between paleo-$CO_2$ and SIs of these two genera, their results demonstrate that the background paleo-$CO_2$ values are around 350–540 ppm between the Late Cretaceous and the Early Tertiary. All lie within the ranges predicted by a long-term geochemical carbon cycle modeling (Berner and Kothavala, 2001) and paleo-$CO_2$ reconstructed from pedogenic carbonates (Ekart et al., 1999), demonstrating a congruence between the estimates based on paleobotany and nonbiological proxies. Immediately above the KTB, the SI of fossil fronds of a fern aff. *Stenochlaena* have extremely low SIs in comparison to fronds of modern *Stellaria palustris* suggesting a much higher atmospheric paleo-$CO_2$ level of at least ~2300 ppm. This indicates an increase of about 1900 ppmv within 10,000 years following the KTB (Beerling et al., 2002). However, the assumption that the low SI values reflect a very high paleo-$CO_2$ level must be considered cautiously. The highly elevated paleo-$CO_2$ just after the extinction event is based on the fern SI, whereas the background paleo-$CO_2$ is based on *Ginkgo*. The sharp paleo-$CO_2$ variation across the KTB should be treated as provisional due to the less than ideal situation of plant sample availability (Beerling et al., 2002).

Accepting this distinctive paleo-$CO_2$ change, a global biogeochemical carbon cycle model shows that the two phenomena, e.g. volcanic $CO_2$ outgassing from the eruption of the Deccan Traps and the carbonate vaporization by a bolide impact are both likely to have been involved in the post-KTB paleo-$CO_2$ increase. It shows that there would have to be 6400–13,000 Gt of $CO_2$ gasified from the carbonate terrace into the atmospheric carbon reservoir by the impact event. This is largely in accordance with the magnitude derived from the calculations (O'Keefe and Ahrens, 1989) but greater than the range of 350 to 3500 Gt $CO_2$ derived from geophysical model studies of the Chicxulub impact (Pope et al., 1997; Pierazzo et al., 1998). Their results suggest that the paleo-$CO_2$ reached its maximum immediately after the impact event.

In contrast to the results of both geochemical modeling and plant stomatal indices, paleosol studies show that paleo-$CO_2$ might have even declined, instead of increased, at the KTB (Nordt et al., 2002, 2003). Applying the paleosol barometer, stable carbon isotope analyses on 40 pedogenic carbonate nodules from Alberta, Canada, indicate extreme fluctuations between 77 and 63 Ma (Nordt et al., 2002, 2003). Paleosol data indicate that the paleo-$CO_2$ rose dramatically from 780 ppm in the Maastrichtian to 1440 ppm near the KTB, but declined sharply to 760 ppm at the boundary (Nordt et al., 2002). A similar paleo-$CO_2$ pattern was also found across the KTB in the Tornillo Basin of Texas, USA, based on paleosol stable carbon isotopes (Nordt et al., 2003). It is argued that the paleo-$CO_2$ drawdown at the KTB might reflect a cessation of volcanic activity in Deccan Plateau, India, and coincides with coeval collapse of marine planktonic productivity (Nordt et al. (2002)).

The age and duration of the Deccan trap volcanism remain highly controversial. Dating of the basalts based on various methods yields ages ranging from ca. 65 Ma to ca. 69 Ma, suggesting that eruption of the traps spanned or was prior to the KTB (Duncan and Pyle, 1988; Allègre et al., 1999; Hofmann et al., 2000; Rao and Lehmann, 2011). Furthermore, the planktonic productivity collapse at the KTB may not have been as extensive as previously thought. A recent study of deep-sea records from the Pacific, Southeast Atlantic, and Southern Oceans demonstrates that phytoplankton-dependent benthic foraminifera did not suffer significant extinction (Alegret et al., 2012). Because of the two sources of paleosol carbon, atmospheric $CO_2$ and biological $CO_2$, the seasonal and climatic biases of paleosol barometer-derived atmospheric paleo-$CO_2$ may be unreliable unless these two kinds of carbon can be distinguished (Breecker et al., 2009, 2010; Royer, 2010). Finally, it should be noted that a paleosol indicates the existence of a geological unconformity (Demko et al., 2004; Retallack, 2008), so that it is often difficult to estimate the duration of the hiatus and the age of the paleosol. A paleosol-based reconstruction of KTB paleo-$CO_2$ fluctuations should be supported by comprehensive barometer calibration and appropriate age constraints.

## 5. Paleo-$CO_2$ and the variability of Cretaceous greenhouse climates

The Cretaceous represents a classic greenhouse climate period in Earth history. During this time, the warm climate was equably distributed around the world. The polar regions were much warmer than today. There were no polar ice sheets. Instead, thermophilic floras and faunas spread to high latitudes. The latitudinal temperature gradient was much lower than today. This general picture of a Cretaceous climate is depicted by Frakes et al. (1992) and Francis and Frakes (1993). However, the trends and shorter-term variations of atmospheric $CO_2$ suggest that the Cretaceous climate was far from unvarying as previously thought (Sloan and Barron, 1990).

We now know that large and rapid climate perturbations occurred during the "greenhouse world" of the Cretaceous, with short-term paleo-$CO_2$ level changes (Jenkyns, 2003). These suggest that the greenhouse conditions may have been transient rather than persistent

(Retallack, 2009a). Long-term changes in atmospheric $CO_2$ levels were forced by magmatism and tectonic activity (Jahren, 2002). The idea of an equable, greenhouse climate throughout the Cretaceous has become suspect for a variety of reasons (Frakes et al., 1992; Wallmann, 2001; Gröcke et al., 2005; Kessels et al., 2006).

It is widely accepted that paleo-$CO_2$ is a primary driver of Phanerozoic climate (Royer et al., 2004; Royer, 2010). The broad picture of climate and $CO_2$ variation through the Phanerozoic shows that warming trends are accompanied by increasing $CO_2$ levels, whereas cooler periods are associated with reductions of atmospheric $CO_2$ (Retallack (2001)). A high level of atmospheric $CO_2$ is thought to be responsible for the warm climates of the Cretaceous (Francis and Frakes, 1993). However, paleo-$CO_2$ levels in the Cretaceous were variable. Evidence from both paleobotany and paleosols demonstrate not only the general trends of paleo-$CO_2$, but also the short-term fluctuations in some intervals (Fig. 1).

Oxygen isotopes of marine fossils indicated that the early Cretaceous was cool, the mid-Cretaceous hot, and the late Cretaceous warm (Huber et al., 2002). Both stomatal and pedogenic carbonate analyses demonstrate generally lower paleo-$CO_2$ levels in the Early Cretaceous, especially in Berriasian, Valanginian and Barremian to Aptian (Fig. 1). This paleo-$CO_2$ level is consistent with suggestions of overall cooler climate and extensive deposits of ice-rafted detritus at high latitudes during the Early Cretaceous (Frakes et al., 1992; Podlaha et al., 1998; Wallmann, 2001; Robinson et al., 2002; Alley and Frakes, 2003; McArthur et al., 2007; Huang et al., 2012). During the Cretaceous the global sea level fluctuated by more than 50 m and it has been proposed that from time to time there were polar ice sheets (Stoll and Schrag, 1996; Hay, 2008; Keller, 2008; Price and Nunn, 2010). The fluctuations of seawater paleotemperatures have been confirmed by several studies (Veizer et al., 2000; Wallmann, 2001; Came et al., 2007). A general cooling prevailed during the Early Cretaceous, from the Berriasian through the Valanginian with the coolest temperatures in the early Hauterivian. Subsequent warming peaked during the mid-Cretaceous (Podlaha et al., 1998; Veizer et al., 2000; Huber et al., 2002; Kessels et al., 2006; Keller, 2008). This variation of paleotemperature coincides with the decreasing trend of atmospheric $CO_2$ levels from the early-middle Berriasian to the early Valanginian and a rise in the late Barremian.

During the middle Cretaceous, from late Albian to Cenomanian and early Turonian, paleo-$CO_2$ levels show a distinct increase, with several short-term fluctuations (Fig. 1). This indicates a generally hot mid-Cretaceous climate condition, consistent with the extreme warmth evidenced by the deep-sea paleotemperature record (Huber et al., 2002). The rapid paleo-$CO_2$ increase during the Cenomanian–Turonian interval (Fig. 1) corresponds to the Cenomanian–Turonian Thermal Maximum. During this time the equatorial Atlantic may have experienced an extremely hot climate with temperatures up to 42 °C (Bice et al., 2006). A sharp $CO_2$ decrease occurred during the Cenomanian to Turonian transition (Fig. 1). It is reflected by a short climate cooling event, which may correspond to one of the possible brief glacial episodes in the Cretaceous greenhouse world proposed by Miller et al. (1999, 2005), Stoll and Schrag (2000), and Price (1999).

The Late Cretaceous was a transition period during which the biosphere evolved from the Mesozoic towards a Cenozoic aspect. Geochemical data show that warmer conditions prevailed during much of the Late Cretaceous with exception of brief (~3 Ma) episodes of cooling, in the mid-Cenomanian and mid-Turonian as mentioned above, and Maastrichtian (Royer, 2006). However, the interval from Cenomanian to Santonian appears to have been a time of quite variable climate as there is conflicting evidence for both warming and cooling (Francis and Frakes, 1993).

The Global Mean Land Surface Temperature (GMLST) trend during the Late Cretaceous varies as interpreted from the oxygen- and carbon-isotopic records. GMLST(ΔT) is the difference from today's GMST, generally taken to be 15 °C. The GMLST(ΔT) increased from ~3 °C in late Cenomanian to ~4.7 °C in mid Turonian, and then dramatically fell to ~2.2 °C in mid-Coniacian. From the Santonian onward, it appears that the GMLST declined gradually with some variations (Wan et al., 2011).

Our analysis indicates that paleo-$CO_2$ levels were relatively low during the Coniacian to Campanian interval (around ca. 500 ppmv or less), although there were two short $CO_2$ fluctuations (Fig. 1). There was a distinct cooling trend and both ocean and land temperatures dropped considerably. Stomatal data show a GMLST decline, suggesting a cooling by about ~1.9 to 1.2 °C (Wan et al., 2011). In the late Campanian, a sharp $CO_2$ spike is recorded in Northeastern China based on high resolution stomatal analysis (Quan et al., 2009). The paleo-$CO_2$ fluctuation in the late Campanian corresponds to the extensive regional development of tuff (Quan et al., 2009). In the global context, a short-term sea water warming in the late Campanian is indicated by isotope records of both planktonic and benthic foraminifera (Abramovich et al., 2003). The late Campanian paleo-$CO_2$ fluctuation correlates with global warming. The latest part of the Maastrichtian appears to have been especially cool, with low temperatures, even freezing, at high latitudes and overall conditions similar to those of the Early Cretaceous (Francis and Frakes, 1993).

## 6. Summary and prospects

This paper synthesizes the $CO_2$ variations throughout the Cretaceous to contribute to understanding its contribution to global warming in deep time. The results indicate that $CO_2$ concentrations remained at a relatively high level throughout the Cretaceous, but at lower levels in the early Cretaceous, higher in the mid-Cretaceous and with a gentle decline during the late Cretaceous. These trends were punctuated at several intervals by rapid paleo-$CO_2$ changes often associated with critical events, such as OAEs and the KTB.

However, although the available data largely suggest the $CO_2$ concentration is coupled to temperature during the Cretaceous, their exact relationship remains uncertain. Temporal resolution due to the length of the quiet magnetic zone in the middle part of the Cretaceous is one of the obstacles that prevent us from a comprehensive understanding of the $CO_2$-climate linkage. But paleo-$CO_2$ determinations and climatic data extracted from sediments intercalated with volcanic rocks will yield a better understanding of the relation between $CO_2$ fluctuations, climatic change, and geological events. In the meanwhile, other potential driving forces or feedbacks such as the widely released sulfur dioxide from extensive volcanic eruptions should not be overlooked in the study of Cretaceous climates.

## Acknowledgments

This is one of the contributions for the “Cretaceous Oceanic Red Beds (CORBs)”collection. We thank Dr. Timothy Horscroft for the kind invitation and encouragement of the work. Prof. Chengshan Wang (China University of Geosciences, Beijing), Prof. Xiumian Hu and Prof. Xianghui Li (Nanjing University) are acknowledged for their kind support and helpful comments on the manuscript. Prof. William W. Hay is appreciated for his helpful linguistic corrections and suggestions of the manuscript revision. We also thank the reviewers for providing constructive suggestion on the manuscript.

The present study was jointly supported by the State Basic Research Program of China (973 Program) (2012CB822003), the National Natural Science Foundation of China (Grant Nos. 41272010, 41002004, and 41372002), the Knowledge Innovation Program of the Chinese Academy of Sciences (Grant No. KZCX2-YW-154) and the Team Program of Scientific Innovation and Interdisciplinary Cooperation of Chinese Academy of Sciences.

## References


Abramovich, S., Keller, G., Stüben, D., Berner, Z., 2003. Characterization of late Campanian and Maastrichtian planktonic foraminiferal depth habitats and vital activities based on stable isotopes. Palaeogeogr. Palaeoclimatol. Palaeoecol. 202, 1–29.

Alegret, L., Thomas, E., Lohmann, K.C., 2012. End-Cretaceous marine mass extinction not caused by productivity collapse. Proc. Natl. Acad. Sci. 109 (3), 728–732.

Allègre, C.J., Birck, J.L., Capmas, F., Courtillot, V., 1999. Age of the Deccan traps using $^{187}Re$–$^{187}Os$ systematics. Earth Planet. Sci. Lett. 170 (3), 197–204.

Alley, N.F., Frakes, L.A., 2003. First known Cretaceous glaciation: Livingston Tillite member of the Cadna-owie formation, South Australia. Aust. J. Earth Sci. 50 (2), 139–144.

Alvarez, L.W., Alvarez, W., Asaro, F., Michael, H.V., 1980. Extraterrestrial cause for the Cretaceous–Tertiary extinction-experimental results and theoretical interpretation. Science 208, 1095–1108.

Arens, N.C., Jahren, A.H., Amundson, R., 2000. Can $C_3$ plants faithfully record the carbon isotopic composition of atmospheric carbon dioxide? Paleobiology 26, 137–164.

Arthur, M.A., Dean, W.E., Pratt, L.M., 1988. Geochemical and climatic effects of increased marine organic carbon burial at the Cenomanian–Turonian boundary. Nature 335, 714–717.

Barclay, R.S., McElwain, J.C., Sageman, B.B., 2010. Carbon sequestration activated by a volcanic $CO_2$ pulse during Ocean Anoxic Event 2. Nat. Geosci. 3, 205–208.

Beerling, D.J., 1996. Ecophysiological responses of woody plants to past $CO_2$ concentrations. Tree Physiol. 16, 389–396.

Beerling, D.J., Chaloner, W.G., 1993. Evolutionary responses of stomatal density to global $CO_2$ change. Biol. J. Linn. Soc. 48 (4), 343–353.

Beerling, D.J., Royer, D.L., 2002. Reading a $CO_2$ signal from fossil stomata. New Phytol. 153 (3), 387–397.

Beerling, D.J., Royer, D.L., 2011. Convergent Cenozoic $CO_2$ history. Nat. Geosci. 4 (7), 418–420.

Beerling, D.J., Lomax, B.H., Royer, D.L., Upchurch Jr., G.R., Kump, L.R., 2002. An atmospheric $pCO_2$ reconstruction across the Cretaceous–Tertiary boundary from leaf megafossils. Proc. Natl. Acad. Sci. 99 (12), 7836–7840.

Benton, M.J., 1995. Diversification and extinction in the history of life. Science 268, 52–58.

Bergman, N.M., Lenton, T.M., Watson, A.J., 2004. COPSE: a new model of biogeochemical cycling over Phanerozoic time. Am. J. Sci. 304 (5), 397–437.

Berner, R.A., 1991. A model for atmospheric $CO_2$ over Phanerozoic time. Am. J. Sci. 291 (4), 339–376.

Berner, R.A., 1994. GEOCARB II: a revised model of atmospheric $CO_2$ over Phanerozoic time. Am. J. Sci. 294 (1), 56–91.

Berner, R.A., 1997. The rise of plants and their effect on weathering and atmospheric. Science 276, 544–546.

Berner, R.A., 2004. The Phanerozoic carbon cycle: $CO_2$ and $O_2$. Oxford University Press, Oxford.

Berner, R.A., 2006. GEOCARBSULF: a combined model for Phanerozoic atmospheric $O_2$ and $CO_2$. Geochim. Cosmochim. Acta 70, 5653–5664.

Berner, R.A., Kothavala, Z., 2001. GEOCARB III: a revised model of atmospheric $CO_2$ over Phanerozoic time. Am. J. Sci. 301 (2), 182–204.

Berner, R.A., Lasaga, A.C., Garrels, R.M., 1983. The carbonate-silicate geochemical cycle and its effect on atmospheric carbon dioxide over the past 100 million years. Am. J. Sci. 283 (9), 641–683.

Bice, K.L., Norris, R.D., 2002. Possible atmospheric $CO_2$ extremes of the middle Cretaceous (late Albian–Turonian). Paleoceanography 17 (4), 1070.

Bice, K.L., Birgel, D., Meyers, P.A., Dahl, K., Hinrichs, K.-U., Norris, R.D., 2006. A multiple proxy and model study of Cretaceous upper ocean temperatures and atmospheric $CO_2$ concentrations. Paleoceanography 21, PA2002.

Birks, H.H., Eide, W., Birk, H.J.B., 1999. Early Holocene atmospheric $CO_2$ concentrations. Science 286, 1815a.

Boucot, A.J., Gray, J., 2001. A critique of Phanerozoic climatic models involving changes in the $CO_2$ content of the atmosphere. Earth Sci. Rev. 56 (1–4), 1–159.

Breecker, D.O., Sharp, Z.D., McFadden, L.D., 2009. Seasonal bias in the formation and stable isotopic composition of pedogenic carbonate in modern soils from central New Mexico, USA. Geol. Soc. Am. Bull. 121 (3–4), 630–640.

Breecker, D.O., Sharp, Z.D., McFadden, L.D., 2010. Atmospheric $CO_2$ concentrations during ancient greenhouse climates were similar to those predicted for A.D. 2100. Proc. Natl. Acad. Sci. 107 (2), 576–580.

Came, R.E., Eiler, J.M., Veizer, J., Azmy, K., Brand, U., Weidman, C.R., 2007. Coupling of surface temperatures and atmospheric $CO_2$ concentrations during the Palaeozoic era. Nature 449, 198–201.

Cerling, T.E., 1984. The stable isotopic composition of modern soil carbonate and its relationship to climate. Earth Planet. Sci. Lett. 71, 229–240.

Cerling, T.E., 1991. Carbon dioxide in the atmosphere: evidence from Cenozoic and Mesozoic Paleosols. Am. J. Sci. 291 (4), 377–400.

Cerling, T.E., 1992. Use of carbon isotopes in paleosols as an indicator of the $P(CO_2)$ of the paleoatmosphere. Global Biogeochem. Cycles 6, 307–314.

Cerling, T.E., 1999. Stable carbon isotopes in palaeosol carbonates. In: Thirty, M., Coincon, R. (Eds.), Palaeoweathering, Palaeosurfaces, and Related Continental Deposits. The International Association of Sedimentologist Special Publication, Oxford, vol. 27, pp. 43–60.

Cerling, T.E., Quade, J., 1993. Stable carbon and oxygen isotopes in soil carbonates. In: Swart, P.K., Lohmann, K.C., McKenzie, J.A., Savin, S.M. (Eds.), Climate Change in Continental Isotopic Records. Geophysical Monograph Series, 78, pp. 217–231.

Cerling, T.E., Quade, J., Wang, Y., Bowman, J.R., 1989. Carbon isotopes in soils and palaeosols as ecology and palaeoecology indicators. Nature 341, 138–139.

Chen, L.Q., Li, C.S., Chaloner, W.G., Beerling, D.J., Sun, Q.G., Collinson, M.E., Mitchell, P.L., 2001. Assessing the potential for the stomatal characters of extant and fossil *Ginkgo* leaves to signal atmospheric $CO_2$ change. Am. J. Bot. 88 (7), 1309–1315.

Cojan, L., Moreau, M.-G., Stott, L., 2000. Stable isotope stratigraphy of the Paleogene pedogenic series of southern France as a basis for continental-marine correlation. Geology 28, 259–262.

Courtillot, V.E., Besse, J., Vandamme, D., Montogny, R., Jaeger, J.J., Capetta, H., 1986. Deccan flood basalts at the Cretaceous/Tertiary boundary? Earth Planet. Sci. Lett. 80, 361–374.

Davis, A., Kemp, A.E.S., Pike, J., 2009. Late Cretaceous seasonal oceanic variability from the Antarctic. Nature 460, 254–258.

DeConto, R.M., Pollard, D., 2003. Rapid Cenozoic glaciation of Antarctica induced by declining atmospheric $CO_2$. Nature 421, 245–249.

Demko, T.M., Currie, B.S., Nicoll, K.A., 2004. Regional paleoclimatic and stratigraphic implications of paleosols and fluvial/overbank architecture in the Morrison Formation (Upper Jurassic), Western Interior, USA. Sediment. Geol. 167 (3–4), 115–135.

Duncan, R.A., Pyle, D.G., 1988. Rapid eruption of the Deccan flood basalts at the Cretaceous/Tertiary boundary. Nature 333, 841–843.

Dworkin, S.I., Nordt, L., Atchley, S., 2005. Determining terrestrial paleotemperatures using the oxygen isotopic composition of pedogenic carbonate. Earth Planet. Sci. Lett. 237 (1–2), 56–68.

Ekart, D.D., Cerling, T.E., Montañez, I.P., Tabor, N.J., 1999. A 400 million year carbon isotope record of pedogenic carbonate: implications for paleoatmospheric carbon dioxide. Am. J. Sci. 299 (10), 805–827.

Erba, E., 1994. Nannofossils and superplumes: the Early Aptian "nannoconid crisis". Paleoceanography 9 (3), 483–501.

Erba, E., 2004. Calcareous nannofossils and Mesozoic oceanic anoxic events. Mar. Micropaleont. 52, 85–106.

Erbacher, J., Thurow, J., 1997. Influence of oceanic anoxic events on the evolution of mid-Cretaceous radiolaria in the North Atlantic and western Tethys. Mar. Micropaleont. 30, 139–158.

Fletcher, B.J., 2006. Environmental Controls on the Carbon Isotope Fractionation of Bryophytes, and Its Significance for Interpreting their Fossil Record. Ph.D. Thesis University of Sheffield, Sheffield, UK.

Fletcher, B.J., Beerling, D.J., Chaloner, W.G., 2004. Stable carbon isotopes and the metabolism of the terrestrial Devonian organism Spongiophyton. Geobiology 2 (2), 107–119.

Fletcher, B.J., Brentnall, S.J., Quick, W.P., Beerling, D.J., 2006. BRYOCARB: a process-based model of thallose liverwort carbon isotope fractionation in response to $CO_2$, $O_2$, light and temperature. Geochim. Cosmochim. Acta 70 (23), 5676–5691.

Fletcher, B.J., Brentnall, S.J., Anderson, C.W., Berner, R.A., Beerling, D.J., 2008. Atmospheric carbon dioxide linked with Mesozoic and early Cenozoic climate change. Nat. Geosci. 1, 43–48.

Frakes, L.A., Francis, J.E., Syktus, J., 1992. Climate Modes of the Phanerozoic. Cambridge University Press, New York (285 pp.).

Francis, J.E., Frakes, L.A., 1993. Cretaceous climates. In: Wright, Paul (Ed.), Sedimentology Review/1. Blackwell Scientific Publications, Oxford, pp. 17–30.

Ghosh, P., Bhattacharya, S., Jani, R., 1995. Palaeoclimate and palaeovegetation in central India during the Upper Cretaceous based on stable isotope composition of the palaeosol carbonates. Palaeogeogr. Palaeoclimatol. Palaeoecol. 114, 285–296.

Ghosh, P., Eiler, J., Campana, S.E., Feeney, R.F., 2007. Calibration of the carbonate "clumped isotope" paleothermometer for otoliths. Geochim. Cosmochim. Acta 71, 2736–2744.

Greenwood, D.R., Scarr, M.J., Christophel, D.C., 2003. Leaf stomatal frequency in the Australian tropical rainforest tree *Neolitsea dealbata* (Lauraceae) as a proxy measure of atmospheric $pCO_2$. Palaeogeogr. Palaeoclimatol. Palaeoecol. 196 (3–4), 375–393.

Gröcke, D.R., Hesselbo, S.P., Jenkyns, H.C., 1999. Carbon-isotope composition of Lower Cretaceous fossil wood: ocean-atmosphere chemistry and relation to sea-level change. Geology 27, 155–158.

Gröcke, D.R., Price, G.D., Robinson, S.A., Baraboshkin, E.Y., Mutterlose, J., Ruffell, A.H., 2005. The Upper Valanginian (Early Cretaceous) positive carbon-isotope event recorded in terrestrial plants. Earth Planet. Sci. Lett. 240 (2), 495–509.

Hansen, K.W., Wallmann, K., 2003. Cretaceous and Cenozoic evolution of seawater composition, atmospheric $O_2$ and $CO_2$: a model perspective. Am. J. Sci. 303, 94–148.

Haq, B.U., Hardenbol, J., Vail, P.R., 1987. Chronology of fluctuating sea level since Triassic (250 million years ago to present). Science 235, 1156–1167.

Haworth, M., Hesselbo, S.P., McElwain, J.C., Robinson, S.A., Brunt, J.W., 2005. Mid-Cretaceous $pCO_2$ based on stomata of the extinct conifer *Pseudofrenelopsis* (Cheirolepidiaceae). Geology 33 (9), 749–752.

Haworth, M., Heath, J., McElwain, J.C., 2010. Differences in the response sensitivity of stomatal index to atmospheric $CO_2$ among four genera of Cupressaceae conifers. Ann. Bot. 105 (3), 411–418.

Haworth, M., Fitzgerald, A., McElwain, J.C., 2011. Cycads show no stomatal-density and index response to elevated carbon dioxide and subambient oxygen. Aust. J. Bot. 59 (7), 630–639.

Hay, W.W., 2008. Evolving ideas about the Cretaceous climate and ocean circulation. Cretac. Res. 29 (5–6), 725–753.

Heimhofer, U., Hochuli, P.A., Herrle, J.O., Andersen, N., Weissert, H., 2004. Absence of major vegetation and palaeoatmospheric $pCO_2$ changes associated with Oceanic Anoxic Event 1a (Early Aptian, SE France). Earth Planet. Sci. Lett. 223, 303–318.

Hemming, N.G., Hanson, G.N., 1992. Boron isotopic composition and concentration in modern marine carbonates. Geochim. Cosmochim. Acta 56 (1), 537–543.

Hofmann, C., Féraud, G., Courtillot, V., 2000. $^{40}Ar/^{39}Ar$ dating of mineral separates and whole rocks from the Western Ghats lava pile: further constraints on duration and age of the Deccan traps. Earth Planet. Sci. Lett. 180 (1–2), 13–27.

Hsü, K.J., He, Q., McKensie, J.A., Weissert, H., Perch-Nielsen, K., Oberhansli, H., Kelts, K., Labreque, J., Tauxe, L., Kranenbuhl, U., et al., 1982. Mass mortality and its environmental and evolutionary consequences. Science 216, 249–256.

Hu, X., Jansa, L., Wang, C., Sarti, M., Bak, K., Wagreich, M., Michalik, J., Soták, J., 2005. Upper Cretaceous oceanic red beds (CORBs) in the Tethys: occurrences, lithofacies, age, and environments. Cretac. Res. 26, 3–20.

Hu, X., Jansa, L., Sarti, M., 2006. Mid-Cretaceous oceanic red beds in the Umbria–Marche Basin, Central Italy: constraints on paleoceanography and paleoclimate. Palaeogeogr. Palaeoclimatol. Palaeoecol. 233, 163–186.
Hu, X., Wang, C., Scott, R.W., Wagreich, M., Jansa, L. (Eds.), 2009. Cretaceous Oceanic Red Beds: Stratigraphy, Composition, Origins, and Palaeoceanographic and Palaeoclimatic Significance: SEPM Special Publication, 91 (276 pp.).
Huang, C.M., Retallack, G.J., Wang, C.S., 2012. Early Cretaceous atmospheric $pCO_2$ levels recorded from pedogenic carbonates in China. Cretac. Res. 33, 42–49.
Huber, B.T., Norris, R.D., MacLeod, K.G., 2002. Deep-sea paleotemperature record of extreme warmth during the Cretaceous. Geology 30, 123–126.
Jahren, A.H., 2002. The biogeochemical consequences of the mid-paleotemperature superplume. J. Geodyn. 34 (2), 177–191.
Jenkyns, H.C., 1999. Mesozoic anoxic events and palaeoclimate. Zentralblatt für Geologie und Paläontologie, Teil 1, 943–949.
Jenkyns, H.C., 2003. Evidence for rapid climate change in the Mesozoic–Palaeogene greenhouse world. Phil. Trans. R. Soc. A 361, 1885–1916.
Johnson, K.R., Nichols, D.J., Attrep Jr., M., Orth, C.J., 1989. High-resolution leaf-fossil record spanning the Cretaceous–Tertiary boundary. Nature 340, 708–711.
Kahniann, J.A., Driese, S.G., 2008. Paleopedology and geochemistry of Late Mississippian (Chesterian) Pennington Formation paleosols at Pound Gap, Kentucky, USA: implications for high-frequency climate variations. Palaeogeogr. Palaeoclimatol. Palaeoecol. 259 (4), 357–381.
Keller, G., 2008. Cretaceous climate, volcanism, impacts, and biotic effects. Cretac. Res. 29 (5–6), 754–771.
Kent-Corson, M.L., Sherman, L.S., Mulch, A., Chamberlain, C.P., 2006. Cenozoic topographic and climatic response to changing tectonic boundary conditions in western North America. Earth Planet. Sci. Lett. 252 (3–4), 453–466.
Kessels, K., Mutterlose, J., Michalzik, D., 2006. Early Cretaceous (Valanginian–Hauterivian) calcareous nannofossils and isotopes of the northern hemisphere: proxies for the understanding of Cretaceous climate. Lethaia 39 (2), 157–172.
Konrad, W., Roth–Nebelsick, A., Grein, M., 2008. Modelling of stomatal density response to atmospheric $CO_2$. J. Theor. Biol. 253 (4), 638–658.
Kouwenberg, L.L.R., McElwain, J.C., Kürschner, W.M., Wagner, F., Beerling, D.J., Mayle, F.E., Visscher, H., 2003. Stomatal frequency adjustment of four conifer species to historical changes in atmospheric $CO_2$. Am. J. Bot. 90 (4), 610–619.
Kürschner, W.M., Kvaček, Z., 2009. Oligocene-Miocene $CO_2$ fluctuations, climatic and palaeofloristic trends inferred from fossil plant assemblages in central Europe. Bull. Geosci. 84 (2), 189–202.
Kürschner, W.M., Stulen, I., Wagner, F., Kuiper, P.J.C., 1998. Comparison of palaeobotanical observations with experimental data on the leaf anatomy of durmast oak [*Quercus petraea* (Fagaceae)] in response to environmental change. Ann. Bot. 81 (5), 657–664.
Kürschner, W.M., Kvaček, Z., Dilcher, D.L., 2008. The impact of Miocene atmospheric carbon dioxide fluctuations on climate and the evolution of terrestrial ecosystems. Proc. Natl. Acad. Sci. 105 (2), 449–453.
Leckie, R.M., Bralower, T.J., Cashman, R.C., 2002. Oceanic anoxic events and plankton evolution: biotic response to tectonic forcing during the mid-Cretaceous. Paleoceanography 17 (3) 13-1–13-29.
Lee, Y.I., 1999. Stable isotopic composition of calcic paleosol of the Early Cretaceous Hasandong Formation, southeastern Korea. Palaeogeogr. Palaeoclimatol. Palaeoecol. 150 (1–2), 123–133.
Lee, Y.I., Hisada, K.I., 1999. Stable isotopic composition of pedogenic carbonates of the Early Cretaceous Shimonoseki Subgroup, western Honshu, Japan. Palaeogeogr. Palaeoclimatol. Palaeoecol. 153 (1–4), 127–138.
Leier, A., Quade, J., DeCelles, P., Kapp, P., 2009. Stable isotopic results from paleosol carbonate in South Asia: paleoenvironmental reconstructions and selective alteration. Earth Planet. Sci. Lett. 279, 242–254.
McArthur, J.M., Janssen, N.M.M., Reboulet, S., Leng, M.J., Thirlwall, M.F., van de Schootbrugge, B., 2007. Palaeotemperatures, polar ice-volume, and isotope stratigraphy (Mg/Ca, $\delta^{18}O$, $\delta^{13}C$, $^{87}Sr/^{86}Sr$): The Early Cretaceous (Berriasian, Valanginian, Hauterivian). Palaeogeogr. Palaeoclimatol. Palaeoecol. 248, 391–430.
McElwain, J.C., 1998. Do fossil plants signal palaeoatmospheric $CO_2$ concentration in the geological past? Philos. Trans. R. Soc. B 353, 83–96.
McElwain, J.C., Chaloner, W.G., 1995. Stomatal density and index of fossil plants track atmospheric carbon dioxide in the Palaeozoic. Ann. Bot. 76, 389–395.
McElwain, J.C., Beerling, D.J., Woodward, F.I., 1999. Fossil plants and global warming at the Triassic–Jurassic boundary. Science 285, 1386–1390.
McElwain, J., Willis, K.J., Lupia, R., 2005. Cretaceous $CO_2$ decline and the radiation and diversification of angiosperms. In: Ehleringer, J.R., Cerling, T.E., Dearing, M.D. (Eds.), A History of Atmospheric $CO_2$ and its Effects on Plants, Animals, and Ecosystems. Springer-Verlag, Berlin, pp. 133–165.
McIver, E.E., 1999. Paleobotanical evidence for ecosystem disruption at the Cretaceous–Tertiary boundary from Wood Mountain, Saskatchewan, Canada. Can. J. Earth Sci. 36 (5), 775–789.
Miller, K.G., Barrera, E., Olsson, R.K., Sugarman, P.J., Savin, S.M., 1999. Does ice drive early Maastrichtian eustasy? Geology 27 (9), 783–786.
Miller, K.G., Kominz, M.A., Browning, J.V., James, D., Mountain, G.S., Katz, M.E., Sugarman, P.J., Cramer, B.S., Christie-Blick, N.S.F., Pekar, S.F., 2005. The Phanerozoic record of global sea-level change. Science 310, 1293–1298.
Montañez, I.P., Tabor, N.J., Niemeier, D., DiMichele, W.A., Frank, T.D., Fielding, C.R., Isbell, J.L., Birgenheier, L.P., Rygel, M.C., 2007. $CO_2$-forced climate and vegetation instability during late Palaeozoic deglaciation. Science 315, 87–91.
Nichols, D.J., Johnson, K.R., 2008. Plants and the K–T Boundary. Cambridge University Press, Cambridge (292 pp.).
Nordt, L., Atchley, S., Dworkin, S.I., 2002. Paleosol barometer indicates extreme fluctuations in atmospheric $CO_2$ across the Cretaceous–Tertiary boundary. Geology 30 (8), 703–706.
Nordt, L., Atchley, S., Dworkin, S.I., 2003. Terrestrial evidence for two greenhouse events in the latest Cretaceous. GSA Today 13 (12), 4–9.
Nordt, L., Orosz, M., Driese, S., Tubbs, J., 2006. Vertisol carbonate properties in relation to mean annual precipitation: implications for paleoprecipitation estimates. J. Geol. 114 (4), 501–510.
Ocampo, A., Vajda, V., Buffetaut, E., 2006. Unraveling the Cretaceous–Paleogene (KT) turnover, evidence from flora, fauna and geology. In: Cockell, C., Gilmour, I., Koeberl, C. (Eds.), Biological Processes Associated with Impact Events: Impact Studies. Springer, Berlin, pp. 197–219.
Officer, C.B., Hallam, A., Drake, C.L., Devine, J.D., 1987. Late Cretaceous and paroxysmal Cretaceous/Tertiary extinctions. Nature 326, 143–149.
O'Keefe, J.D., Ahrens, T.J., 1989. Impact production of $CO_2$ by the Cretaceous/Tertiary extinction bolide and the resultant heating of the Earth. Nature 338, 247–249.
Pagani, M., Arthur, M.A., Freeman, K.H., 1999. Miocene evolution of atmospheric carbon dioxide. Paleoceanography 14 (3), 273–292.
Pagani, M., Zachos, J.C., Freeman, K.H., Tipple, B., Bohaty, S., 2005. Marked decline in atmospheric carbon dioxide concentrations during the Paleogene. Science 309, 600–603.
Passalia, M.G., 2009. Cretaceous $pCO_2$ estimation from stomatal frequency analysis of gymnosperm leaves of Patagonia, Argentina. Palaeogeogr. Palaeoclimatol. Palaeoecol. 273 (1–2), 17–24.
Passey, B.H., Cerling, T.E., Perkins, M.E., Voorhies, M.R., Harris, J.M., Tucker, S.T., 2002. Environmental change in the Great Plains: an isotopic record from fossil horses. J. Geol. 110, 123–140.
Pearson, P.N., Foster, G.L., Wade, B.S., 2009. Atmospheric carbon dioxide through the Eocene–Oligocene climate transition. Nature 461, 1110–1113.
Pierazzo, E., Kring, D.A., Melosh, H.J., 1998. Hydrocode simulation of the Chicxulub impact event and the production of climatically active gases. J. Geophys. Res. 103 (E12), 28607–28625.
Podlaha, O.G., Mutterlose, J., Veizer, J., 1998. Preservation of $\delta^{18}O$ and $\delta^{13}C$ in belemnite rostra from the Jurassic/Early Cretaceous successions. Am. J. Sci. 298, 324–347.
Pope, K.O., Baines, K.H., Ocampo, A.C., Ivanov, B.A., 1997. Energy, volatile production, and climatic effects of the Chicxulub Cretaceous/Tertiary impact. J. Geophys. Res. 102 (E9), 21645–21664.
Price, G.D., 1999. The evidence and implications of polar ice during the Mesozoic. Earth Sci. Rev. 48 (3), 183–210.
Price, G.D., Nunn, E.V., 2010. Valanginian isotope variation in glendonites and belemnites from Arctic Svalbard: transient glacial temperatures during the Cretaceous greenhouse. Geology 38 (3), 251–254.
Prochnow, S.J., Nordt, L.C., Atchley, S.C., Hudec, M.R., 2006. Multi-proxy paleosol evidence for middle and late Triassic climate trends in eastern Utah. Palaeogeogr. Palaeoclimatol. Palaeoecol. 232 (1), 53–72.
Quade, J., Cerling, T.E., Bowman, J.R., 1989. Systematic variations in the carbon and oxygen isotopic composition of pedogenic carbonate along elevation transects in the southern Great Basin, United States. Geol. Soc. Am. Bull. 101, 464–475.
Quan, C., Sun, C., Sun, Y., Sun, G., 2009. High resolution estimates of paleo-$CO_2$ levels through the Campanian (Late Cretaceous) based on *Ginkgo* cuticles. Cretac. Res. 30 (2), 424–428.
Quan, C., Sun, G., Zhou, Z., 2010. A new Tertiary *Ginkgo* (Ginkgoaceae) from the Wuyun Formation of Jiayin, Heilongjiang, northeastern China and its paleoenvironmental implications. Am. J. Bot. 97 (3), 446–457.
Rao, N.V.C., Lehmann, B., 2011. Kimberlites, flood basalts and mantle plumes: new insights from the Deccan large igneous province. Earth Sci. Rev. 107 (3–4), 315–324.
Retallack, G.J., 2001. A 300-million-year record of atmospheric carbon dioxide from fossil plant cuticles. Nature 411, 287–290.
Retallack, G.J., 2005. Pedogenic carbonate proxies for amount and seasonality of precipitation in paleosols. Geology 33 (4), 333–336.
Retallack, G.J., 2008. Soils of the Past: An Introduction to Paleopedology. Wiley-Blackwell, Oxford (520 pp.).
Retallack, G.J., 2009a. Refining a pedogenic-carbonate $CO_2$ paleobarometer to quantify a middle Miocene greenhouse spike. Palaeogeogr. Palaeoclimatol. Palaeoecol. 281 (1–2), 57–65.
Retallack, G.J., 2009b. Greenhouse crises of the past 300 million years. Geol. Soc. Am. Bull. 121 (9–10), 1441–1455.
Retallack, G.J., Huang, C.M., 2011. Ecology and evolution of Devonian trees in New York, USA. Palaeogeogr. Palaeoclimatol. Palaeoecol. 299 (1–2), 110–128.
Robinson, S.A., Andrews, J.E., Hesselbo, S.P., Radley, J.D., Dennis, P.F., Harding, I.C., Allen, P., 2002. Atmospheric $pCO_2$ and depositional environment from stable isotope geochemistry of calcrete nodules (Barremian, Lower Cretaceous, Wealden Beds, England). J. Geol. Soc. 159, 215–224.
Romanek, C., Grossman, E., Morse, J., 1992. Carbon isotopic fractionation in synthetic aragonite and calcite: effects of temperature and precipitation rate. Geochim. Cosmochim. Acta 56 (1), 419–430.
Royer, D.L., 2001. Stomatal density and stomatal index as indicators of paleoatmospheric $CO_2$ concentration. Rev. Palaeobot. Palynol. 114, 1–28.
Royer, D.L., 2003. Estimating latest Cretaceous and Tertiary atmospheric $CO_2$ from stomatal indices. In: Wing, S.L., Gingerich, P.D., Schmitz, B., Thomas, E. (Eds.), Causes and Consequences of Globally Warm Climates in the Early Paleogene. The Geological Society of America, Boulder, pp. 79–93.
Royer, D.L., 2006. $CO_2$-forced climate thresholds during the Phanerozoic. Geochim. Cosmochim. Acta 70, 5665–5675.
Royer, D.L., 2008. Linkages between $CO_2$, climate, and evolution in deep time. Proc. Natl. Acad. Sci. 105 (2), 407–408.
Royer, D.L., 2010. Fossil soils constrain ancient climate sensitivity. Proc. Natl. Acad. Sci. 107 (2), 517–518.
Royer, D.L., Berner, R.A., Beerling, D.J., 2001a. Phanerozoic atmospheric $CO_2$ change: evaluating geochemical and paleobiological approaches. Earth Sci. Rev. 54 (4), 49–392.

Royer, D.L., Wing, S., Beerling, D.J., Jolley, D.W., Koch, P.L., Hickey, L.J., Berner, R.A., 2001b. Paleobotanical evidence for near present day levels of atmospheric $CO_2$ during part of the Tertiary. Science 292, 2310–2313.
Royer, D.L., Berner, R.A., Montañez, I.P., Tabor, N.J., Beerling, D.J., 2004. $CO_2$ as a primary driver of Phanerozoic climate. GSA Today 14 (3), 4–10.
Royer, D.L., Berner, R.A., Park, J., 2007. Climatic sensitivity constrained by $CO_2$ concentrations over the past 420 million years. Nature 446, 530–532.
Salisbury, E.J., 1927. On the causes and ecological significance of stomatal frequency with special reference to woodland flora. Philos. Trans. R. Soc. Lond. Ser. B 216, 1–65.
Schlanger, S.O., Jenkyns, H.C., 1976. Cretaceous oceanic anoxic events: causes and consequences. Geol. Mijnb. 55 (3–4), 79–184.
Sheldon, N.D., Tabor, N.J., 2009. Quantitative paleoenvironmental and paleoclimatic reconstruction using palaeosols. Earth Sci. Rev. 95 (1–2), 1–52.
Sheldon, N.D., Retallack, G.J., Tanaka, S., 2002. Geochemical climofunctions from North American soils and application to paleosols across the Eocene–Oligocene boundary in Oregon. J. Geol. 110 (6), 687–696.
Sinha, A., Stott, L.D., 1994. New atmospheric $pCO_2$ estimates from paleosols during the late Paleocene/early Eocene global warming interval. Glob. Planet. Chang. 9, 297–307.
Sloan, L.C., Barron, E.J., 1990. Equable climates during earth history? Geology 18, 489–492.
Stoll, H.M., Schrag, D.P., 1996. Evidence for glacial control of rapid sea level changes in the early Cretaceous. Science 272, 1771–1774.
Stoll, H.M., Schrag, D.P., 2000. High-resolution stable isotope records from the Upper Cretaceous rocks of Italy and Spain: glacial episodes in a greenhouse planet? Geol. Soc. Am. Bull. 112 (2), 308–319.
Sun, B.N., Xiao, L., Xie, S.P., Deng, S.H., Wang, Y.D., Jia, H., Turner, S., 2007. Quantitative analysis of paleoatmospheric $CO_2$ level based on stomatal characters of fossil *Ginkgo* from Jurassic to Cretaceous in China. Acta Geol. Sin. Engl. Ed. 81 (6), 931–939.
Tajika, E., 1999. Carbon cycle and climate change during the Cretaceous inferred from a biogeochemical carbon cycle model. Island Arc 8, 293–303.
Tanner, L.H., Hubert, J.F., Coffey, B.P., McInerney, D.P., 2001. Stability of atmospheric $CO_2$ levels across the Triassic/Jurassic boundary. Nature 411, 675–677.
Tarduno, J.A., Brinkman, D.B., Renne, P.R., Cottrell, R.D., Scher, H., Castillo, P., 1998. Evidence for extreme climatic warmth from Late Cretaceous Arctic vertebrates. Science 282, 2241–2243.
Tschudy, R.H., Pillmore, C.L., Orth, C.J., Gilmore, J.S., Knight, J.D., 1984. Disruption of the terrestrial plant ecosystem at the Cretaceous–Tertiary boundary, western Interior. Science 225, 1030–1032.
Uhl, D., Herp, H., 2005. Variability of stomatal density and index in the Upper Permian conifer *Quadrocladus* Mädler — a taphonomical case study. Palaeogeogr. Palaeoclimatol. Palaeoecol. 218, 205–215.
van Bentum, E.C., Reichart, G.-J., Forster, A., Sinninghe Damsté, J.S., 2011. Latitudinal differences in the amplitude of the OAE-2 carbon isotopic excursion: $pCO_2$ and paleoproductivity. Biogeosciences. 8 (3), 6191–6226.
van Hoof, T.B., Wagner-Cremer, F., Kürschner, W.M., Visscher, H., 2008. A role for atmospheric $CO_2$ in preindustrial climate forcing. Proc. Natl. Acad. Sci. 105, 15815–15818.
Veizer, J., Godderis, Y., François, L.M., 2000. Evidence for decoupling of atmospheric $CO_2$ and global climate during the Phanerozoic eon. Nature 408, 698–701.
Wagner, F., Dilcher, D.L., Visscher, H., 2005. Stomatal frequency responses in hardwood-swamp vegetation from Florida during a 60-year continuous $CO_2$ increase. Am. J. Bot. 92 (4), 690–695.
Wagreich, M., Hu, X.M., Sageman, B., 2009a. Causes of oxic–anoxic changes in Cretaceous marine environments and their implications for earth systems — an introduction. Sediment. Geol. 235, 1–4.
Wagreich, M., Neuhuber, S., Egger, J., Wendler, I., Scott, R.W., Malata, E., Sanders, D., 2009b. Cretaceous oceanic red beds (CORBs) in the Austrian Eastern Alps: passive margin vs. active-margin depositional settings. In: Hu, X.M., Wang, C.S., Scott, R.W., Wagreich, M., Jansa, L. (Eds.), Cretaceous Oceanic Red Beds: Stratigraphy, Composition, Origins, Palaeoceanographic, and Palaeoclimatic Significance. SEPM Special Publication, 91. Society for Sedimentary Geology, Tulsa, OK, pp. 37–91.
Wallmann, K., 2001. Controls on the Cretaceous and Cenozoic evolution of seawater composition, atmospheric $CO_2$ and climate. Geochim. Cosmochim. Acta 65 (18), 3005–3025.
Wan, C.B., Wang, D.H., Zhu, Z.P., Quan, C., 2011. Trend of Santonian (Late Cretaceous) atmospheric $CO_2$ and global mean land surface temperature: evidence from plant fossils. Sci. China Earth Sci. 54 (9), 1338–1345.
Wang, C.S., Hu, X.M., 2005. Cretaceous world and oceanic red beds. Earth Sci. Front. 12 (2), 11–21 (in Chinese with English abstract).
Wang, C.S., Hu, X.M., Sarti, M., Scott, R.W., Li, X.H., 2005. Upper Cretaceous oceanic red beds in southern Tibet: a major change from anoxic to oxic, deep-sea environments. Cretac. Res. 26, 21–32.
Wang, C.S., Hu, X.M., Huang, Y.J., Wagreich, M., Scott, R., Hay, W., 2011. Cretaceous oceanic red beds as possible consequence of oceanic anoxic events. Sediment. Geol. 235 (1–2), 27–37.
Weissert, H., Erba, E., 2004. Volcanism, $CO_2$ and palaeoclimate: a Late Jurassic–Early Cretaceous carbon and oxygen isotope record. J. Geol. Soc. Lond. 161, 695–702.
Wellman, C.H., 2010. The invasion of the land by plants: when and where? New Phytol. 188 (2), 306–309.
Wellman, C.H., Osterloff, P.L., Mohiuddin, U., 2003. Fragments of the earliest land plants. Nature 425, 282–285.
White, P.D., Schiebout, J., 2008. Paleogene paleosols and changes in pedogenesis during the initial Eocene thermal maximum: Big Bend National Park, Texas, USA. Geol. Soc. Am. Bull. 120, 1347–1361.
Wilf, P., Johnson, K.R., 2004. Land plant extinction at the end of the Cretaceous: a quantitative analysis of the North Dakota megafloral record. Paleobiology 30 (3), 347–368.
Woodward, F.I., 1987. Stomatal numbers are sensitive to increases in $CO_2$ from pre-industrial levels. Nature 327, 617–618.
Wynn, J.G., 2007. Carbon isotope fractionation during decomposition of organic matter in soils and paleosols: implications for paleoecological interpretations of palaeosols. Palaeogeogr. Palaeoclimatol. Palaeoecol. 251, 437–448.
Yapp, C.J., Poths, H., 1992. Ancient atmospheric $CO_2$ pressures inferred from natural goethites. Nature 355, 342–344.